

# <sup>1</sup> Supplementary figures Capturing regeneration in models of forest <sup>2</sup> dynamics

Olalla Díaz-Yáñez, Yannek Käber, Tim Anders, Friedrich Bohn,  
Kristin H. Braziunas, Josef Brůna, Rico Fischer, Samuel M. Fischer,  
Jessica Hetzer, Thomas Hickler, Christian Hochauer, Manfred J. Lexer,  
Heike Lischke, Mats Mahnken, Paola Mairotta, Ján Merganič,  
Katarina Merganičová, Tobias Mette, Marco Mina, Xavier Morin,  
Werner Rammer, Christopher P.O. Reyer, Simon Scheiter, Daniel Scherrer,  
Harald Bugmann

2023-04-28

11 Contents

12	<b>1 Supplementary Material 1: Model reports</b>	<b>2</b>
13	1.1 4C . . . . .	2
14	1.2 ForCEEPS & ForCEEPS(f) . . . . .	4
15	1.3 FORMIND . . . . .	5
16	1.4 ForClim 1 & ForClim 11 . . . . .	7
17	1.5 SIBYLA . . . . .	8
18	1.6 xComp . . . . .	11
19	1.7 PICUS . . . . .	13
20	1.8 iLand . . . . .	15
21	1.9 LandClim . . . . .	17
22	1.10 Landis II . . . . .	18
23	1.11 TreeMig . . . . .	22
24	1.12 LPJ-GUESS . . . . .	25
25	1.13 aDGVM2 . . . . .	28
26	<b>2 Supplementary Material 2: Supplementary figures and tables</b>	<b>32</b>
27	2.1 Ingrowth levels, tree diversity and mortality in tree establishment . . . . .	32
28	2.2 Model traits and model performance . . . . .	39
29	2.3 Total ingrowth and individual species regeneration niches . . . . .	41
30	2.4 References . . . . .	43

<sup>31</sup> **1 Supplementary Material 1: Model reports**

<sup>32</sup> **1.1 4C**

<sup>33</sup> **1.1.1 Authors**

<sup>34</sup> Mahnken M., Gutsch M., Reyer C.P.O., Lasch-Born P.

<sup>35</sup> **1.1.2 Model**

<sup>36</sup> The most complete reference resource for the 4C (v2.2) model and regeneration module is:

- <sup>37</sup> • Lasch-Bonn et al. 2020. Description and evaluation of the process-based forest model 4C v2.2 at four  
<sup>38</sup> European forest sites. DOI: <https://doi.org/10.5194/gmd-13-5311-2020>)

<sup>39</sup> **1.1.3 Climate**

<sup>40</sup> We used the provided daily ERA5-CHELSA climate data set and complemented the CHELSA time series  
<sup>41</sup> data regarding relative humidity with the model after [Eccel et al. \(2012\)](#) based on minimum and mean daily  
<sup>42</sup> temperature to accomodate data needs of 4C. The missing data for January 2nd and 3rd 2013 were filled  
<sup>43</sup> with data from January 1st and 4th 2013 respectively. For construction of longer climate time series we  
<sup>44</sup> looped through the provided time series from 1981 to 2018 up to the maximum simulation length of 2500  
<sup>45</sup> years. We amended situations where leap year inconsistencies arised by removing February 29 or duplicating  
<sup>46</sup> data from February 28. Otherwise, the unaltered daily data were used to run 4C on a daily basis. We  
<sup>47</sup> applied a constant atmopsheric CO<sub>2</sub> concentration of 380 ppm.

<sup>48</sup> **1.1.4 Soil**

<sup>49</sup> We used parametrized soils readily available for 4C from the EU soil data base. The link from parametrized  
<sup>50</sup> soil to soil quality was done by extracting the plant available water storage capacity as the model bucket size  
<sup>51</sup> of the rooted soil horizons. We excluded bucket size values of lower than 10 cm and larger than 35 cm. The  
<sup>52</sup> bucket size was reprojected to the range from 0 to 1. In addition we tested the sensitivity of dominant tree  
<sup>53</sup> height at age 100 years for monospecific stands of all five species simulated to the available soils using model  
<sup>54</sup> simulations with 4C. The dominant tree height at age 100 years was then also reprojected to the range from  
<sup>55</sup> 0 to 1 in order to derive a model specific soil quality indicator for all paramterized soils. Then we multiplied  
<sup>56</sup> this relative model specific soil quality with the relative soil quality derived from the bucket size to the range  
<sup>57</sup> from 1 to 5. The match between paramterized soil and plot was then done by finding the pair of soil quality  
<sup>58</sup> with the minimum difference between simuation protocol prescribed soil quality and the soil quality of the  
<sup>59</sup> paramterized soils as described above.

<sup>60</sup> **1.1.5 Topography**

<sup>61</sup> Topographical information was not considered in the simulations.

<sup>62</sup> **1.1.6 Tree species**

<sup>63</sup> We initialized stands with five out of the eleven proposed species/genera: *Fagus sylvatica* (fasy), *Picea*  
<sup>64</sup> *abies* (piab), *Betula* spp. (betu; 4C parameters for *Betula pendula*), *Quercus* spp. (quer; 4C parameters  
<sup>65</sup> for *Quercus robur*) and *Pinus sylvestris* (pisy) since only these are fully parameterized for an application  
<sup>66</sup> as proposed in the simulation protocol. Each plot was initialized with all five tree species with similar

67 distributions of height classes and number of individuals: 2000 individuals/ha with height around 0.25 m,  
68 1000 individuals/ha with height around 0.75 m and 500 individuals/ha with height around 1.75 m. In  
69 total 17500 individuals/ha. *Carpinus betulus*, *Tilia cordata*, *Acer pseudoplatanus*, *Fraxinus excelsior*, *Alnus*  
70 *glutinosa* and *Abies alba* are not fully parameterized in 4C.

### 71 1.1.7 Simulations

72 **1.1.7.1 Dispersal and seed input** There is no explicitly modelled seed dispersal in a stand and between  
73 stands. We applied a constant sapling establishment rate every five years of 2000 individuals/ha for all five  
74 species; 10000 individuals/ha in total every five years. The constant sapling establishment provides constant  
75 regeneration potential if favorable conditions for sapling growth (especially light and water regime) are  
76 present. This approach enables regeneration of other species than only those present in the stand to establish  
77 if competition allows. The resulting recruitment patterns are an outcome of the dynamical processes from  
78 the sapling stage onward. Seed production and germination were not explicitly simulated.

79 **1.1.7.2 Simulation length and equilibrium criteria** To reach equilibrium and obtain dynamics in  
80 the equilibrium period, we simulated a maximum of 2500 years. 4C is usually applied for much shorter  
81 simulation periods and different technical as well as model-theory related issues arise when simulating longer  
82 than 100-150 years. Therefore 2500 years can be seen as the upper limit of continuous simulation in the  
83 defined simulation setup. The first 500 years were not sampled for recruitment as we assume the model needs  
84 this time to reach equilibrium. In this long simulation period 4C partially projects unrealistically large tree  
85 heights resulting in premature termination of the simulation (36 plots) so that not all plots were simulated  
86 for the full 2500 years. We started sampling the recruits after the first 500 simulation years from non-  
87 overlapping 10 year periods to obtain 200 samples. For shorter simulation periods we produced 200 samples  
88 from overlapping 10 year periods. In addition, we excluded those plots in which 4C simulated unrealistically  
89 high basal area values of over 150 m<sup>2</sup> (19 plots). We used this large threshold to give the model maximum  
90 flexibility to explore the solution space in these long simulation runs although we acknowledge that this is  
91 an unrealistic overestimation that is probably originating from misrepresented density dependent mortality  
92 processes in long simulation runs and misrepresented single tree dimensions due to wrong assumptions of  
93 tree geometry and biomass share of such old-aged individuals. Furthermore those plots with less than 1000  
94 simulation years (16 plots) before termination were excluded because the sample space after the first 500  
95 years was too small. Additionally we included another subset criterion removing all samples that have a  
96 ba > 90 to exclude unrealistically high samples without the need to exclude the full site. This resulted in  
97 discarding 0.8 % of the samples.

### 98 1.1.8 Outputs

99 We provide 200 samples each for 48 plots and at least 190 samples each for 117 plots while not simulating  
100 35 plots (see reason for excluded plots in “Simulation length and equilibrium criteria”). These stem from  
101 10 year periods that overlap partially (for < 2500 simulation years) or do not overlap (for 2500 simulation  
102 years). The number of recruits (r.trees) is the sum of individuals that cross the threshold diameter (7/10  
103 cm) in the 10 year sample period per hectare that have not already died until the sample year. The recruit's  
104 basal area (r.ba) is the sum of the basal area per hectare of the trees that cross the diameter threshold that  
105 have not already died until the sample year. The total stand basal area (ba) is the basal area per hectare of  
106 all trees in the stand > 0 cm diameter at breast height (no lower boundary) at the sample time per species.  
107 We provide the data for both diameter thresholds, 7 and 10 cm. In over 90 % of the decades no recruitment  
108 takes place.

109 **4C (v2.2)** is usually not used for simulations of forest equilibrium dynamics, potential natural vegetation  
110 assessment and long simulation periods but rather shorter-term simulations (up to 100-150 years). In addition,  
111 only five species out of the pool of eleven potentially relevant species here are parameterized in 4C so  
112 that projections of the potential natural vegetation done with 4C need to be considered in the light of model  
113 uncertainty. For example, the spatial homogeneity in the model leads to cyclic recruitment patterns. When

114 the adult stands dies of, young individuals are recruited into the larger diameter classes because more light  
115 reaches lower canopy layer since larger (adult) trees do not anymore prevent the light reaching lower canopy  
116 layers. This results in increased growth of the regeneration layer during those times. In most stands *Fagus*  
117 *sylvatica* dominates the stand after some time but occasionally individuals of other species, like *Picea abies*  
118 or *Quercus* spp. cross the recruitment diameter threshold.

## 119 **1.2 ForCEEPS & ForCEEPS(f)**

### 120 **1.2.1 Author**

121 Xavier Morin & François de Coligny

### 122 **1.2.2 Model**

123 The most complete reference resource for the ForCEEPS & ForCEEPS(f) model and regeneration module  
124 are:

- 125 • Morin X., de Coligny F., Bugmann H., Limousin J.-M., Ourcival J.-M., Martin-StPaul N., Simioni  
126 G., Cailleret M., Prevosto B., Toïgo M., Vennetier M., Cateau E., Guillemot J. 2021. Beyond forest  
127 succession: a gap model to study ecosystem functioning and tree community composition under climate  
128 change. *Functional Ecology*. 35, 955-975.
- 129 • Jourdan M., Dreyfus, P., Riond C., Cordonnier T., Cornet B., de Coligny F., Morin X. 2021. Man-  
130 aging mixed stands can mitigate severe climate change impacts on French alpine forests. *Regional  
131 Environmental Change*. 21, 78.
- 132 • Morin X., Damestoy T., Toïgo M., Jactel H., Castagneyrol B. Meredieu C. 2020. Using forest gap  
133 models and experimental data to explore long-term effects of tree diversity on the productivity of  
134 mixed planted forests. *Annals of Forest Science*. 77 <https://doi.org/10.1007/s13595-020-00954-0>.

### 135 **1.2.3 Climate**

136 ForCEEPS requires monthly data. A 4000-yr long time-series was obtained for each site by randomizing  
137 available years from the CHELSA database, with mean monthly temperature and monthly sum of precipi-  
138 tations (see 1.2.2).

### 139 **1.2.4 Soil**

140 Soil quality is represented by a continuous value between 1 and 5, as provided (see 1.2.3) Soil Field Capacity  
141 (SFC) was assessed as follows:  $SFC = 8 + (X-1)*(25-8)/(5-1)$ , in which X is the ‘soil\_qual’ value in the  
142 provided ‘soil\_quality\_200.csv’ file.

### 143 **1.2.5 Topography**

144 Not considered.

145 **1.2.6 Simulations**

146 In each site, the simulation consists of 4000 yr-long simulation of 1ha of forest (ie. 10 patches of 1000 m<sup>2</sup>),  
147 starting from bare-ground. There was no dispersal between patches. Two kinds of simulations have been  
148 carried out in each of the 200 sites. In a first set of simulations, regeneration dynamics was simulated with  
149 a seed rain from a potential species list, thus independent from the actual forest composition, as classically  
150 done in gap models. Under this design, a number of seedling is randomly chosen for each patch, and a species  
151 identity is randomly sorted from a potential species list (defined at the start of simulation) assigned to each  
152 seedling. Then each seedling tries to colonize the site depending on whether the suitability between species  
153 requirements and site conditions (climate, light, soil quality, browsing index). In a second set of simulations,  
154 regeneration dynamics was simulated with a seed rain whose composition depended on the actual forest  
155 composition. Under this design, a number of seedling is randomly chosen for each patch, but the species  
156 identity is assigned according to species relative abundance (calculated across all 10 patches according to  
157 species biomass). For instance, if at year i the adult trees of species j represent 60% of the total biomass  
158 across the 10 patches, then 60% of the seedlings that try to colonize the patches at year i will belong to  
159 species j. Then, similarly to the first design, each seedling tries to colonize the site depending on whether  
160 the suitability between species requirements and site conditions. In the two sets of simulations, simulations  
161 have been run for both thresholds for regeneration (7 and 10 cm).

162 **1.2.7 Outputs**

163 Outputs consisted in species specific regeneration rates per decade and per ha, by considering the last 2000  
164 years of simulations to ensure that pseudo-equilibrium state is reached. Results were aggregated for every 10  
165 years for the last 2000 years at the 1ha-level. Variables: - Site: numbers corresponding to the climate data  
166 file - Sample: one per decade, for a total of 2000 years = identified from 1 to 200 - Species: name specified  
167 as requested (eg. 'fasy') - r.trees: number of trees outcrossing the threshold (7 or 10 cm) during the decade,  
168 for the 10 patches simulated (= 1ha), per species - r.ba: summed basal area of the r.trees, per species - ba:  
169 summed basal area of all trees per species at the end of the decade - dbh: threshold used

170 **1.3 FORMIND**

171 **1.3.1 Authors**

172 Samuel M. Fischer, Friedrich Bohn, Rico Fischer

173 **1.3.2 Model**

174 A full description of the model can be found in Fischer et al (2016) . The basis for the parameterization we  
175 applied is described in Bohn et al (2014):

- 176 • Bohn, F. J., Frank, K., & Huth, A. (2014). Of climate and its resulting tree growth: Simulating  
177 the productivity of temperate forests. Ecological Modelling, 278, 9–17. <https://doi.org/10.1016/j.ecolmodel>.
- 178
- 179 • Fischer, R., Bohn, F., Dantas de Paula, M., Dislich, C., Groeneveld, J., Gutiérrez, A. G., Kazmierczak,  
180 M., Knapp, N., Lehmann, S., Paulick, S., Pütz, S., Rödig, E., Taubert, F., Köhler, P., & Huth, A.  
181 (2016).Lessons learned from applying a forest gap model to understand ecosystem and carbon dynamics  
182 of complex tropical forests. Ecological Modelling, 326, 124–133. <https://doi.org/10.1016/j.ecolmodel>.  
183 2015.

184 **1.3.3 Climate**

185 To incorporate climate, we used the data set ‘daily\_era5\_chelsa\_200.csv’, which contains climate data on a  
186 daily resolution. We considered the covariates precipitation, temperature, and irradiance, the latter of which  
187 we converted to units used in Formind. Adding on to these data, we used a constant and site-independent  
188 potential evapotranspiration (PET) value of  $4 \frac{\text{mm}}{\text{d}}$  and assumed that the mean day length was 12h at all  
189 sites.  
190 Since we simulated longer time periods than the 38 years for which we had climate data, we used the provided  
191 data in a randomized fashion. For each simulation year, we applied the climate data of a randomly selected  
192 year. We neglected the existence of leap years, which led to a minor time shift in climate data of later years.

193 **1.3.4 Soil**

194 We modelled soil conditions by using the provided soil quality values as proxy for soil depth. To that end,  
195 we scaled the provided values to the typical range of soil depth values used in Formind for temperate forests.  
196 Specifically, we multiplied the soil quality values by factor 0.5 to obtain the modelled soil depth in meters.

197 **1.3.5 Topography**

198 We did not use any topography data.

199 **1.3.6 Tree species**

200 We considered each of the 11 species in the protocol explicitly. We chose the model parameters for the  
201 individual species based on the work by Bohn et al (2014). For species that were not covered by Bohn et al  
202 (2014), we used parameter values of similar species with known parameters. The species composition was  
203 not predefined and evolved solely from the seed input and the model dynamics.

204 **1.3.7 Simulations**

205 **1.3.7.1 Simulation area** We simulated a forest area of 1ha, which was divided into 25 patches of size  
206  $20\text{m} \times 20\text{m}$ . No interactions between trees from different patches were considered in the model. That is, the  
207 25 patches were independent replicates of one another.

208 **1.3.7.2 Seed generation and dispersal** We modelled seed generation as global external seed rain.  
209 Specifically, we assumed that for each species, there is a constant seed inflow of  $250 \frac{\text{seeds}}{\text{ha}\cdot\text{yr}}$ , which is distributed  
210 evenly among the 25 individual patches. We supposed that all seeds promptly establish to seedlings with  
211 initial stem diameters at breast height (DBH) of 5cm.

212 **1.3.7.3 Simulation length and sampling approach** We started the simulation at each site with a  
213 burn-in phase of 1000 years and collected samples of the output variables in subsequent years. The length of  
214 the burn-in phase was chosen based on earlier experiences with the model. To confirm that the model reached  
215 its limiting behaviour, we plotted the evolution of the output variables (e.g. the basal area) at selected sites  
216 over time and verified that no trends were visible after the burn-in phase.

217 We computed the output variables in equidistant time intervals of 60 years. Before taking a sample, we saved  
218 parts of the model’s state. Then, we simulated the forest for 10 years and computed the output variables,  
219 comparing the model’s current state with the state saved earlier (see below). After taking the sample, we  
220 simulated the forest for another 50 years to reduce correlations between samples. Then, we repeated the  
221 procedure until the desired number of 200 samples was collected.

222 **1.3.8 Outputs**

223 To determine the number and basal area of recruits, we compared the set of large trees before and after  
224 the regeneration time period of 10 years. Prior to simulating the forest for the regeneration time period,  
225 we saved the internal IDs of all trees with DBHs above the thresholds of 0.07m or 0.1m, respectively. We  
226 stored these IDs in set data structures  $S_{0.07}^{\text{prior}}$  and  $S_{0.1}^{\text{prior}}$ , corresponding to one threshold value each. After  
227 the regeneration time, we repeated the procedure, obtaining tree ID sets  $S_{0.07}^{\text{posterior}}$  and  $S_{0.1}^{\text{posterior}}$ . We then  
228 computed the set differences  $S_{0.07}^{\text{recruits}} = S_{0.07}^{\text{posterior}} \setminus S_{0.07}^{\text{prior}}$  and  $S_{0.1}^{\text{recruits}} = S_{0.1}^{\text{posterior}} \setminus S_{0.1}^{\text{prior}}$  and determined both  
229 the number and cumulative basal area of the trees in  $S_{0.07}^{\text{recruits}}$  and  $S_{0.1}^{\text{recruits}}$  by considered species, respectively.  
230 Finally, we computed the total basal area for each considered species by adding up the basal areas of all  
231 corresponding individuals. Note that the initial DBH of seedlings in our model was 0.05m. Consequently,  
232 smaller trees were not included in the basal area computation.

233 **1.4 ForClim 1 & ForClim 11**

234 **1.4.1 Authors**

235 Yannek Käber, Harald Bugmann

236 **1.4.2 Model**

237 The most complete reference resource for the ForClim 1 & ForClim 11 model and regeneration module is:

- 238 • Bugmann, H. (1994). On the ecology of mountainous forests in a changing climate: A simulation  
239 study. Huber, N., Bugmann, H., & Lafond, V. (2020). Capturing ecological processes in dynamic  
240 forest models: Why there is no silver bullet to cope with complexity. *Ecosphere*, 11(5). <https://doi.org/10.1002/ecs2.3109>

242 **1.4.3 Climate**

243 Temperature and precipitation were aggregated to monthly means and sums, respectively, including their  
244 standard deviation. These values served as input for the weather generator within the model. The weather  
245 generator simulates wheather conditions in an annual time step based on the monthly average temperatures  
246 and precipitations sums.

247 **1.4.4 Soil**

248 Soil data were translated to bucket sizes values based on the assumption that the lowest soil quality value of  
249 1 refers to a bucket size of 10 cm and the highest soil quality of 5 refers to a bucket size of 35 cm. Specifically  
250 we used the following formula to calculate the bucket size  $\text{bucket\_size} = 10 + (\text{soil\_quality}-1) / 4 * 25$ .

251 **1.4.5 Topography**

252 Topographic information was included by specifying the kSIAsp parameter. This parameter defines a value  
253 between -2 and 2 which affects the calculated Potential Evapotranspiration within the model. For details on  
254 the calculation of this value see Käber et. al. 2021.

255 **1.4.6 Tree species**

256 All species required were simulated: *Fagus sylvatica*, *Picea abies*, *Abies alba*, *Carpinus betulus*, *Tilia cordata*,  
257 *Acer pseudoplatanus*, *Betula* spp., *Fraxinus excelsior*, *Quercus* spp., *Alnus glutinosa*, *Pinus sylvestris*

258 In addition the following species were simulated: *Acer campestre*, *Acer platanoides*, *Alnus incana*, *Alnus*  
259 *viridis*, *Castanea sativa*, *Corylus avellana*, *Larix decidua*, *Pinus montana*, *Populus nigra*, *Populus tremula*,  
260 *Salix alba*, *Sorbus aria*, *Sorbus aucuparia*, *Taxus baccata*, *Tilia platyphyllos*, *Ulmus glabra*, *Pinus cembra*

261 **1.4.7 Simulations**

262 All simulations were run according to the protocol. For each site we simulated on 16 ha (i.e., 100 patches  
263 of 0.08 ha). We defined a spin up phase of 1000 years. After the spin up we simulated 200 years of forest  
264 dynamics.

265 **1.4.8 Outputs**

266 We sampled in 10 year intervals between the simulation years 1010 to 1200, which resulted in 16 times 20  
267 intervals each with one ha.

268 **1.5 SIBYLA**

269 **1.5.1 Authors**

270 Ján Merganič, Katarína Merganičová, Marek Fabrika, Peter Valent

271 **1.5.2 Model**

272 SIBYLA is the simulator of forest biodynamics. It belongs to the category of semi-empirical tree growth sim-  
273 ulators. It consists of the set of mathematical models and algorithms that are transformed into an integrated  
274 software package SIBYLA Suite. The model has been developed at the Department of Forest Management  
275 and Geodesy, Technical University in Zvolen, Slovakia. The basis of the model was the modelling principle  
276 and algorithms implemented in SILVA 2.2 (Pretzsch 1992, Kahn 1994). The model is sensitive to climatic  
277 factors (length of growing season, mean temperature during growing season, annual temperature amplitude,  
278 and total precipitation during growing season). The climatic factors modify height and diameter growth  
279 potential, and consequently tree increment. The climatic factors also influence tree regeneration model.

280 The most complete reference resource for the SIBYLA model and regeneration module is:

- 281 • Fabrika (2005) "Simulátor biodynamiky lesa SIBYLA." *Koncepcia, konštrukcia a programové riešenie.*  
282 *Habilitačná práca, Technická univerzita vo Zvolene*  
283 • Materials available in <http://etools.tuzvo.sk/sibyla/english/model.htm>.

284 **1.5.3 Climate**

285 We used CHELSEA monthly and daily time series from 1981 to 2018 to derive climate variables necessary  
286 for simulations with SIBYLA as follows: Monthly average temperature (tas) values were used to derive the  
287 SIBYLA site-specific characteristic called the „annual temperature amplitude” (labelled as TAMPL or s5  
288 in the model) that was calculated as a difference between the maximum and minimum monthly average  
289 temperatures. Monthly average temperature (tas) values for months April to September were used to derive  
290 the SIBYLA site-specific characteristic called the „average temperature during the growing season” (labelled

291 as TEMP or s6 in the model). Monthly precipitation sums (pr) for months April to September were summed  
292 up to derive the SIBYLA site-specific characteristic called the „precipitation total during the growing season”  
293 (labelled as PRECIP or s8 in the model). Daily average temperature (tas) values were used to derive the  
294 SIBYLA site-specific characteristic called the „length of the growing season” (labelled as DAYS or s4 in the  
295 model).

#### 296 1.5.4 Soil

297 The information on site-specific soil quality (file name: soil\_quality\_200.csv) was used to define two SIBYLA  
298 site-specific characteristic called the „soil moisture” (labelled as MOIST or s7 in the model) and the „soil  
299 nutrient supply” (labelled as NUTR or s3). Since these two characteristics can obtain values in the range  
300 from 0 to 1, the provided values on soil quality were converted to this range by dividing each value with 5  
301 (the maximum). We used the long-term average of CO<sub>2</sub> concentrations in air that represented the period  
302 1981 – 2018. The long-term average of CO<sub>2</sub> was calculated from the annual CO<sub>2</sub> data obtained from Mauna  
303 Loa observations (Keeling et al. 1976). Similarly, we used the long-term NO<sub>x</sub> concentration representing the  
304 time period 1981-2018. This was obtained by averaging annual values of NO<sub>x</sub> concentration in air calculated  
305 using the equation by Kahn (1994), where the year is the driving variable.

#### 306 1.5.5 Topographyp

307 The growth simulator SIBYLA uses the model of ecological classification applied in the growth simulator  
308 SILVA 2.2, which was derived by Kahn (1994). Site is specified using ecological site characteristics describing  
309 climate, air, and soil, also called site variables:

- 310 • s1 (N2O) ... NO<sub>x</sub> concentration in air (ppb)
- 311 • s2 (CO<sub>2</sub>) ... CO<sub>2</sub> concentration in air (ppm)
- 312 • s3 (NUTR) ... soil nutrient supply (relative value in the range from 0 to 1)
- 313 • s4 (DAYS) ... number of days in the vegetation period (days with daily mean temperature above 10°C)
- 314 • s5 (TAMPL) ... annual temperature amplitude (the difference between minimum and maximum monthly  
315 temperature in °C)
- 316 • s6 (TEMP) ... daily mean temperature in the vegetation period in °C (from April to September)
- 317 • s7 (MOIST) ...soil moisture (relative value in the range from 0 to 1)
- 318 • s8 (PRECIP) ... precipitation amount in the vegetation period in mm (from April to September)
- 319 • s9 (ARID)... aridity index according to de Martone in mm.°C-1 They directly influence the production  
320 capacity of a stand (tree height and diameter increment).

#### 321 1.5.6 Tree species

322 At the beginning of the simulations we determined balanced tree species composition of all 12 tree species  
323 pre-defined in the „Regeneration workshop protocol”. It means that at the beginning each species was  
324 represented by the same volume, mean tree diameter, mean tree height, and age.

#### 325 1.5.7 Simulations

326 The simulations were performed following the “Regeneration workshop protocol”. Hence, we simulated the  
327 pre-defined 200 sites with the model SIBYLA under current climate. The simulations were performed with  
328 the help of two software tools for automatised handling of multiple sites to speed up the process called  
329 DBCreator and Automat (Valent et al. 2018).

330 **1.5.7.1 Simulation area and site** We set the simulation area to 1ha, i.e. each site was represented by  
331 an area of 1 ha, to enable a sufficiently large area for species interactions. Larger areas were not possible due  
332 to the restrictions in the number of trees per plot (the maximum number of trees per plot is 6,000). Due to  
333 the restriction in the maximum number of trees per plot we established a 40-year-old forest stand at each  
334 site with the balanced tree species composition as defined above. We used site-specific elevation and aspect  
335 obtained from the information on topography and elevation (file name: topo\_data\_200.csv).

336 **1.5.7.2 Simulation length** Each site was simulated for 3,000 years. Based on the analysis of the tempo-  
337 ral development of multiple stand variables including number of trees, mean tree and stand characteristics,  
338 the simulation time until the equilibrium was set to 500 years. Hence, the first 500 simulated years were  
339 excluded from the results. The submitted output includes the required information per decade during the  
340 2,500 years.

341 **1.5.7.3 Dispersal** Relevant aspects of the dispersal (if any) and seed input parameters in your model  
342 The regeneration model operates if there are mature trees able to produce seeds. Hence, the initial forest  
343 stand had to be established to allow the reproduction and regeneration module. The seed yield of individual  
344 trees is predicted in relation to species-specific characteristics including tree age interval of seed production  
345 and fertility (age of start, optimum and end), seed production per adult tree, transmission distance, seed  
346 purity, seed quality, germination capacity, absolute weight of seeds. Seed tree production is further modified  
347 with the regulators and reduction factors, which describe other conditions necessary for the germination,  
348 survival, and the establishment of the next generation, e.g. stand canopy closure (Fabrika 2005, Merganič  
349 and Fabrika 2009, Fabrika et. al. 2009, 2011).

### 350 **1.5.8 Outputs**

351 To derive the required information, we worked with the model output for individual trees per decade. First,  
352 we calculated basal area of individual trees from the simulated diameter at breast height using the equation  
353 for the area of a circle. Total basal area (ba) was obtained by summing tree basal areas per species and  
354 decade. The number of recruits (r.trees) per species was derived by counting the trees that exceeded the  
355 diameter threshold (7 or 10 cm) in the specific time. The basal area of recruits (r.ba) per species was  
356 calculated by summing tree basal areas of recruits per species. NA was assigned if no trees of a specific  
357 species occurred in the period.

### 358 **1.5.9 References**

- 359 Fabrika M., Merganič J., Merganičová K., 2009: Natural regeneration density model developed for the  
360 purposes of the individual-tree growth simulator. Acta Facultatis Forestalis Zvolen, 51(3), p. 125-137, ISSN:  
361 0231-5785 Fabrika, M., (2005): Simulátor biodynamiky lesa SIBYLA, koncepcia, konštrukcia a programové  
362 riešenie. Habilitačná práca. Technická univerzita vo  
363 Zvolene, 238 p. Kahn, M., (1994): Modellierung der Höhenentwicklung ausgewählter Baumarten in Ab-  
364 hängigkeit vom Standort. Forstliche Forschungsber. München, Vol. 141, 221 p. Keeling C. D., R. B.  
365 Bacastow, A. E. Bainbridge, C. A. Ekdahl Jr., P. R. Guenther, L. S. Waterman, J. F. S. Chin 1976: At-  
366 mospheric carbon dioxide variations at Mauna Loa Observatory, Hawaii. Tellus. XXVIII, 6: 538-551,  
367 <https://doi.org/10.1111/j.2153-3490.1976.tb00701.x>
- 368 Merganič J., Fabrika M., 2009: Determination of climatic-site strata based on rectified climatic rasters for  
369 the purposes of natural regeneration density model. Acta Facultatis Forestalis Zvolen, 51(3), p. 113-124,  
370 ISSN: 0231-5785
- 371 Merganič, J., Fabrika, M., Merganičová, K., 2011: Submodel of height-diameter function for climatic-site  
372 strata of the model of natural regeneration in the growth simulator SIBYLA. Acta Facultatis Forestalis  
373 Zvolen, 53(1), p.155-168, ISSN: 0231-5785

374 Pretzsch, H., (1992): Konzeption und Konstruktion von Wuchsmodellen für Rein- und Mischbestände.  
375 Forstliche Forschungsberichte München, Nr.115, 358 p. Valent, P., Merganič J., Výboštok J. 2018: Opti-  
376 mus – Software for Multi-criteria analysis. TU Zvolen.

377 **1.6 xComp**

378 **1.6.1 Authors**

379 Tobias Mette, LWF.

380 **1.6.2 Model**

381 The forest growth model xcomp was developed to simulate gap dynamics of monospecific stands with a strong  
382 emphasis on position-dependent individual tree competition. The model consists of three units: (1) the main  
383 growth phase which determines the growth and mortality of each individual tree above 5 cm dbh, (2) the old-  
384 growth phase where individual trees exceeding a certain dbh-limit decline in vitality and eventually die, and  
385 (3) the regeneration phase where seedling growth and mortality is modelled depending on light availability.  
386 The primary focus of the model was to establish a set of robust algorithms that can be flexibly calibrated  
387 for different species attributes. The model was used to simulate single-species stand development cycles for  
388 Nothofagus pumilio in Patagonia (Mette 2014), for European beech in NE-Bavaria (Mette et al. 2016) and a  
389 Norway spruce stand with different mortality algorithms (Bugmann et al. 2019). For the current article the  
390 model was (4) connected to a climate sensitive species distribution model to modify growth and mortality  
391 in dependence of the site conditions, and (5) extended from single to multi-species simulations (c.f. Section  
392 1.6.7).

393 The most complete reference resource for the xComp model and regeneration module are:

- 394 • Mette, T. (2014). xcomp Tutorial (v2014\_08). Technical Report, TUM. DOI: 10.13140/RG.2.2.32524.59529
- 395 • Mette, T. (2014) Using Reineke to self-calibrate mortality in individual tree based forest growth mod-  
396 elling. Beiträge zur Forstwissenschaftlichen Tagung, Dresden, 17.-20.09.2014. 10.13140/RG.2.2.11553.07527

397 **1.6.3 Climate**

398 The species parameterisation in xcomp is sensitive to long-term climate, i.e. 30-year averages of summer  
399 temperature, summer precipitation and winter temperature. Reactions to daily, monthly or periodic extremes  
400 are not implemented as deterministic but as stochastically processes functionally dependent on the long-term  
401 climate. The climate sensitivity of growth, mortality and regeneration is described in Section 1.6.7.

402 **1.6.4 Soil**

403 Soil moisture class MOIST was used to modify the climate sensitivity via summer precipitation PJJA by  
404  $PJJA(mod) = PJJA + 15 * MOIST - 45$  (in mm).

405 **1.6.5 Topography**

406 Topography is no input parameter in xcomp. It may only effect the simulation results indirectly through  
407 climate or soil parameters.

408 **1.6.6 Tree species**

409 From the suggested species spectrum *Alnus glutinosa* and *Fraxinus excelsior* were not included in the species  
410 mix. *Quercus spec* was split into *Q. petraea* and *Q. pubescens*, but united in the validation to meet the  
411 protocol.

412 **1.6.7 Simulations**

413 The simulation was carried out according to the protocol by Bugmann et al. (2022). I.e. the simulation is  
414 initiated for mixed species stands of 1 ha size at 200 sites of with given climate and soil conditions. The  
415 initial species mix consists of up to 10 species of equal shares with an initial root mean square diameter dq of  
416 8 cm. Xcomp simulates forest growth in 5 year intervals. Data are validated after having reached a climate  
417 dependent equilibrium – which is typically the case after 750 years (= 150 simulation periods). Starting  
418 with year 760, data are read out for 200 10 year intervals (until year 2750, simulation period 550). Further  
419 simulation relevant model details:

420 (1) The main growth phase is determined by the processes growth and mortality. Mortality is determined by  
421 the Reineke exponent rke and the stand density sdi and calibrated over a range of 8 cm to 50 cm dq (= root  
422 mean square diameter) so that stem number N equals:  $N = sdi^*(dq/25)^rke$ . A tree's resource acquisition  
423 area res (m<sup>2</sup>) is approximated as  $res = 1e4 / (sdi^*(dbh/25)^rke)$ . As the Reineke exponent is fixed to -1.6,  
424 species with higher/ lower sdi have a lower/ higher resource acquisition area for a given dbh. Potential dbh  
425 growth dd is calculated by multiplying a reference dbh growth with a site specific temperature dependent  
426 modifier. The individual dbh growth in the stand is further modified by the neighbourhood competition.

427 (2) The old growth phase sets in when a tree passes a certain old growth dbh (ogDbh) which depends on  
428 the site conditions. Having passed this threshold dbh a tree is assigned a mortality period that assumes  
429 a value not greater than a site independent maximum ogPer. The maximum old growth time span ranges  
430 from 100 years (birch) to 350 years (fir). During the old growth phase dbh growth declines and more light  
431 becomes available for regeneration.

432 (3) The regeneration phase allows seedling development on a 1x1 m grid over the entire stand. First, a light  
433 availability matrix (1x1 m) is calculated from a cumulative crown shadow which decreases with increasing  
434 distance to the tree center. Next, regeneration matrices (1x1 m) are created for each of the stand's species.  
435 In the initial period, the regeneration matrix of each species is empty, but at the end of each period, a light  
436 dependent dbh growth and mortality is calculated for each 1m raster cell. The dbh growth is scaled so that  
437 under full light 5 cm dbh is reached in a defined regeneration period (regnPer) that depends on the site  
438 conditions. The default value is set to 15 years and equal for all species. Dbh growth is modified by the light  
439 availability and the species' regeneration light demand. This is a decisive difference between the species and  
440 favours shadow-tolerant trees like fir and beech in the absence of large gaps. However, each raster cell is  
441 afflicted with a species bonus or malus that provides local variation to the global regeneration parameters.  
442 Mortality in the regeneration raster occurs as a random process, the likelihood of which depends on the  
443 climate.

444 (4) The climate sensitivity was calculated by methods of species distribution modelling. Effectively species  
445 abundance in European NFI-plots (Mauri et al. 2017) was related to climate of the plots (Karger et al. 2017)  
446 using generalized additive models as in Thurm et al. (2018). Input variables were summer temperature mean  
447 (Jun-Aug), winter temperature mean (Dec-Feb) and summer precipitation sum (Jun-Aug). Abundance was  
448 transformed into prevalence () so that the values for each species can assume a range from 0 to 1. The  
449 prevalence values modify dbh growth dd, old growth dbh ogDbh, the regeneration period regnPer, and the  
450 regeneration mortality regnMort.

451 (5) The extension from single to multiple species simulation introduced no technical changes to the single-  
452 species growth and mortality behaviour. Competition as the main interaction between trees depends on the  
453 crown size and density of the neighbouring trees and can turn out an dis/advantage for one or the other  
454 species. But species calibration parameters were not changed due to mixture-specific interaction.

455 **1.6.8 Outputs**

456 Since the simulation output tables contain all biometric variables on an individual tree basis, all required  
457 outputs can be derived directly from the output tables. Being a very deterministic model what typically  
458 happens in xcomp is that the equilibria consist of one or two species. Shade tolerance favours fir and beech in  
459 the absence of large gaps creating disturbances. The second most important parameter is the site suitability  
460 which is estimated by the modelled species prevalence and affects growth and thereby competitiveness. As  
461 it is the first time that xcomp is used in a multiple species application there is room for improvements.  
462 The automation of a robust calibration of the main growth phase is a precondition to investigate how for  
463 instance larger disturbances, a weighted regeneration potential oriented at the main stand, higher or selective  
464 mortality of the regeneration affect the species composition and turnover.

465 **1.6.9 References**

- 466 Bugmann, H., Seidl, R., Hartig, F., Bohn, F., Brüna, J., Cailleret, M., ... & Reyer, C. P. (2019). Tree  
467 mortality submodels drive simulated long-term forest dynamics: Assessing 15 models from the stand  
468 to global scale. *Ecosphere*, 10(2), e02616.
- 469 Karger, D. N., Conrad, O., Böhner, J., Kawohl, T., Kreft, H., Soria-Auza, R. W., ... & Kessler, M.  
470 (2017). Climatologies at high resolution for the earth's land surface areas. *Scientific data*, 4(1), 1-20.
- 471 Mauri, A., Strona, G., & San-Miguel-Ayanz, J. (2017). EU-Forest, a high-resolution tree occurrence  
472 dataset for Europe. *Scientific data*, 4(1), 1-8.
- 473 Mette, T., Falk, W., Blaschke, M., Förster, B., Walentowski, H. (2016). Modelling natural forest dy-  
474 namics in individual tree based forest growth simulators. *Beiträge zur Forstwissenschaftlichen Tagung*,  
475 Freiburg, 26.-29.09.2016. 10.13140/RG.2.2.29169.15201
- 476 Thurm, E. A., Hernandez, L., Baltensweiler, A., Ayan, S., Rasztovits, E., Bielak, K., ... & Falk, W.  
477 (2018). Alternative tree species under climate warming in managed European forests. *Forest Ecology  
478 and Management*, 430, 485-497.

479 **1.7 PICUS**

480 **1.7.1 Authors**

481 Christian Hochauer, Manfred J. Lexer

482 **1.7.2 Model**

483 The core elements of PICUS are described in Lexer and Hönniger (2001) and Seidl et al. (2005). Specific  
484 details regarding the regeneration module can be found in Woltjer et al. (2008).

- 485 • Lexer MJ, Hönniger K (2001) A modified 3D-patch model for spatially explicit simulation of vegetation  
486 composition in heterogeneous landscapes. *For Ecol Manag* 144:43–65. [doi:10.1016/S0378-1127\(00\)00386-8](https://doi.org/10.1016/S0378-1127(00)00386-8)
- 488 • Seidl R, Lexer MJ, Jäger D, Hönniger K (2005) Evaluating the accuracy and generality of a hybrid  
489 patch model. *Tree Physiol* 25:939–951. [doi:10.1093/treephys/25.7.939](https://doi.org/10.1093/treephys/25.7.939)
- 490 • Woltjer M, Rammer W, Brauner M, Seidl R, Mohren GMJ, Lexer MJ (2008) Coupling a 3D patch  
491 model and a rockfall module to assess rockfall protection in mountain forests. *J Environ Manag*  
492 87:373–388. [doi:10.1016/j.jenvman.2007.01.031](https://doi.org/10.1016/j.jenvman.2007.01.031)

493 **1.7.3 Climate**

494 We used the provided monthly climate data (monthly\_era5\_chelsa\_200.csv). The provided solar radiation  
495 rsds was converted to MJ per m<sup>2</sup>. Additionally, vpd was calculated.

496 **1.7.4 Soil**

497 Based on the provided continuous value for soil quality between 1 and 5 minimum (soil quality = 1) and  
498 maximum (soil quality = 5) values for soil water holding capacity (80mm, 200mm), plant available Nitrogen  
499 (40 kg ha<sup>-1</sup> yr<sup>-1</sup>, 100 kg ha<sup>-1</sup> yr<sup>-1</sup>) and soil pH (4.2, 5.6) were defined. Linear interpolation was used to scale  
500 between the minimum and maximum values.

501 **1.7.5 Topography**

502 Not considered.

503 **1.7.6 Tree species**

504 The species composition was defined by the given species from the protocol: Fagus sylvatica, Picea abies,  
505 Abies alba, Carpinus betulus, Tilia cordata, Acer pseudoplatanus, Betula spp., Fraxinus excelsior, Quercus  
506 spp., Alnus glutinosa and Pinus sylvestris. For Betula spp. Betula pendula was simulated, for Quercus  
507 spp. the species Quercus petraea and Quercus robur where used. The establishment from bare ground was  
508 achieved via external seed input (see also in section seed dispersal), so depending on the environment and  
509 random components all the given species had a chance to grow into the respective simulation. In addition,  
510 on site production of seed is considered depending on age and size of potential parent trees.

511 **1.7.7 Simulations**

512 **1.7.7.1 Simulation Area** In PICUS the area is defined via the number of 10 m by 10 m patches. For  
513 this simulation we used an area of 12 by 12 patches resulting in an area of 1.44 ha. This size of the simulated  
514 forest provides relatively stable species composition & structure and reasonable simulation time.

515 **1.7.7.2 Seed dispersal** For the experiment seed input to the simulated forest happens via 2 pathways:  
516 (1) external seed input to every patch in any simulated year (fixed number of seed per patch per species). (2)  
517 locally produced seed by parent trees growing in the simulated forest. Seed production depends on species,  
518 and tree size and a random component accounting for mast years. Seed dispersal depends on whether a  
519 species is anemochorous or zoochorous. If anemochorous tree height and seed characteristics determine  
520 the maximum dispersal range and the shape of the dispersal function. Based on germination rate, the  
521 environmental factors (temperature, soil moisture, Nitrogen, light) and the amount of seeds in combination  
522 with a random component seedling establishment is calculated per patch in any given year. Seedling cohorts  
523 grow through 4 height classes and are then eventually recruited into the tree population.

524 **1.7.7.3 Simulation length** We decided to use the temporal sampling. We first run the model into a  
525 quasi equilibrium and continue afterwards with another 2000 years. The simulation time until equilibrium  
526 was chosen with 600 years from experience in other projects and a few simulations with test sites where 600  
527 years was a sufficiently long simulation time to reach an equilibrium state.

528 **1.7.8 Output**

529 Output consisted of species-specific regeneration rates per decade and per ha. Oak species were aggregated.  
530 A sample was taken for every 10 years for a total period of 2000 years once the model had reached equilibrium  
531 (see 1.7.7.3). Ingrowth was determined by counting the trees passing the 7cm and 10cm DBH thresholds  
532 every 10 years. Basal area of the ingrowth was determined at the end of each decade.

533 **1.8 iLand**

534 **1.8.1 Authors**

535 Werner Rammer, Kristin Braziunas

536 **1.8.2 Model**

537 The most complete reference resource for the iLand regeneration module is:

- 538 • Seidl, R., Spies, T. a. T. A. T. a., Rammer, W., Steel, E. A. A., Pabst, R. J. R. J. R. J., & Olsen, K.  
539 (2012). Multi-scale Drivers of Spatial Variation in Old-Growth Forest Carbon Density Disentangled  
540 with Lidar and an Individual-Based Landscape Model. *Ecosystems*, 15(8), 1321-1335. <https://doi.org/10.1007/s10021-012-9587-2>

542 **1.8.3 Climate**

543 Climate inputs for iLand are at daily temporal resolution. We used daily climate from the CHELSA dataset  
544 for maximum and minimum temperature, precipitation, and surface shortwave radiation. We calculated  
545 daily vapor pressure deficit (VPD) from these inputs assuming daily minimum temperature is dewpoint  
546 temperature, a reasonable assumption except under very arid conditions (Campbell and Norman 2000). We  
547 calculated vapor pressure from temperature using the Tetens formula with different coefficients for tempera-  
548 tures above or below 0° C (Murray 1967). We then followed methods outlined by the Food and Agriculture  
549 Organization of the United Nations (Allen et al. 1998) to calculate vapor pressure deficit as the difference  
550 between average daily saturation vapor pressure (derived from minimum and maximum temperature) and  
551 ambient vapor pressure derived from dewpoint temperature. Some daily VPD values were negative because  
552 there were days in the CHELSA dataset where minimum temperature exceeded maximum temperature;  
553 negative VPD values were set to 0.

554 As recommended by workshop organizers, we filled in daily values for two missing days in 2013 (Jan 2 and  
555 Jan 3) with daily values for Jan 1 and 4, respectively.

556 Atmospheric CO<sub>2</sub> concentration was set to 380 ppm and latitude was set to 50° N for all sites. Annual  
557 climate year was drawn randomly with replacement from the full dataset (1981-2018) for each site for the  
558 duration of the simulation.

559 **1.8.4 Soil**

560 Inputs for soil depth, texture, and fertility (plant available nitrogen) were extracted from a previously  
561 compiled Europe-wide dataset (unpublished dataset). We averaged values in a 1 km buffer around blurred  
562 site coordinates provided by workshop organizers. Relationships between ranked site quality provided by  
563 workshop organizers and soils data from our Europe-wide dataset were weak (Pearson's |r| ranged from 0.04  
564 to 0.34), but followed expected trends with lower sand content, higher water holding capacity, and higher  
565 fertility associated with higher site quality. Albeit the weak correlation, we chose to use our available data  
566 set because we could avoid additional assumptions as it included all site variables needed for the model.

567 **1.8.5 Topography**

568 Topographic information was not used.

569 **1.8.6 Tree species**

570 Tree composition is defined at the species level. All individually requested species (*Fagus sylvatica*, *Picea*  
571 *abies*, *Abies alba*, *Carpinus betulus*, *Tilia cordata*, *Acer pseudoplatanus*, *Fraxinus excelsior*, *Alnus glutinosa*,  
572 *Pinus sylvestris*) were included. For the two taxa where species was not defined, we identified a representative  
573 species (*Betula pendula* for *Betula* spp. and *Quercus robur* for *Quercus* spp.). No other species were included  
574 in model simulations.

575 **1.8.7 Simulations**

576 **1.8.7.1 Simulation area** The simulation extent for each site was 1000 m x 1000 m (total area = 100  
577 ha). Environmental conditions were homogeneous for each site.

578 **1.8.7.2 Dispersal** Dispersal parameters are species-specific and include maturity age, fecundity (seedling  
579 potential per m<sup>2</sup> crown area), masting (lower seed production in non-mast years), and dispersal distance  
580 (probabilistic dispersal kernel). A small fraction of seeds are dispersed over longer distances (long distance  
581 dispersal algorithm). Dispersal is calculated at 20 m spatial resolution. Seedling establishment is further  
582 modified by other environmental constraints and is stochastically spatially distributed at finer (2 m) reso-  
583 lution. The simulation extent is treated as a spatially explicit landscape, so neighboring cells can serve as  
584 seed sources for each other.

585 We initialized our simulation experiments from bare ground with uniform probability of seed availability set  
586 to a low level (0.001) for all species. Once trees reached maturity, they also contributed to seed availability  
587 and dispersal.

588 **1.8.7.3 Simulation length** Simulations were run for 2010 years, and equilibrium was reached at year  
589 1500. We assessed temporal patterns of species composition and basal area and defined equilibrium as  
590 when forest composition and structure stabilized across all sites (“potential natural vegetation”). Some sites  
591 had high interannual variation, especially in basal area, after equilibrium; this variation did not represent  
592 directional change and appeared instead to be related to sites with extreme growth conditions and variation  
593 in randomly selected annual climate.

594 **1.8.7.4 Simulation approaches** Only one simulation was run per site.

595 **1.8.8 Output**

596 For each site, we generated decadal outputs for the full simulation extent every 100 years after equilibrium  
597 was reached (i.e., 1500-1509, 1600-1609, ..., 2000-2009). This resulted in outputs for a total of 600 ha (100  
598 ha simulation extent x 6 decades). From this list, we randomly sampled 200 ha without replacement.

599 We derived recruit density and basal area annually by species. Trees > 4 m in height are represented as  
600 individuals in iLand, so we were able to identify individual trees that crossed the DBH threshold of either 7  
601 or 10 cm each year. We summed the number of annual recruits and their basal area in the year they crossed  
602 the recruitment threshold for each 10-year output period.

603 We averaged total density and basal area by species for each decade. We further included 0 values (complete  
604 cases) for species that were missing from a given sample and site.

605 **1.8.9 References**

606 Allen, R. G., L. S. Pereira, D. Raes, and M. Smith. 1998. Crop evapotranspiration - Guidelines for computing  
607 crop water requirements. FAO - Food and Agriculture Organization of the United Nations, Irrigation and  
608 drainage paper 56. Campbell, G. S., and J. M. Norman. 2000. An Introduction to Environmental Biophysics.  
609 Springer Science & Business Media. Murray, F. W. 1967. On the computation of saturation vapor pressure.  
610 Journal of Applied Meteorology 6:203–204.

611 **1.9 LandClim**

612 **1.9.1 Authors**

613 Olalla Díaz-Yáñez, Harald Bugmann

614 **1.9.2 Model**

615 We used LandClim version 2.0, which calculates forest dynamics at a decadal time step. The complete  
616 reference resources for the LandClim model and its regeneration module are:

- 617 • SCHUMACHER, S., H. BUGMANN, AND D. J. MLADENOFF. (2004). “Improving the formulation  
618 of tree growth and succession in a spatially explicit landscape model” Ecological Modelling 180: 175-  
619 194.
- 620 • SCHUMACHER, S. AND H. BUGMANN. (2006). “The relative importance of climatic effects, wild-  
621 fires and management for future forest landscape dynamics in the Swiss Alps” Global Change Biology  
622 12: 1435-1450.
- 623 • SCHUMACHER, S., B. REINEKING, J. SIBOLD, AND H. BUGMANN. (2006). “Modeling the  
624 impact of climate and vegetation on fire regimes in mountain landscapes” Landscape Ecology 21:  
625 539-554.
- 626 • Manual available on the model web page: <https://ites-fe.ethz.ch/openaccess/products/landclim>

627 **1.9.3 Climate**

628 Climate inputs for LandClim are at monthly temporal resolution. We used monthly climate from the  
629 CHELSA dataset provided in the protocol, using temperature and precipitation variables. During the sim-  
630 ulations, we randomly sampled the annual climate data from the CHELSA time series.

631 **1.9.4 Soil**

632 We used the soil quality provided in the protocol to infer the Available Water Holding Capacity (WHC)  
633 needed in LandClim. We assigned WHC = 8 cm for soil quality one and WHC = 25 cm for soil quality five,  
634 and interpolated the values for the other categories linearly between these two extremes.

635 **1.9.5 Topography**

636 We used the altitude and soil information provided in the protocol to create 200 landscapes, one per site.  
637 However, each landscape created per site had no slope, altitude, or aspect variation.

638 **1.9.6 Tree species**

639 We simulated forest dynamics considering only the 11 species proposed in the protocol: *Fagus sylvatica*,  
640 *Picea abies*, *Abies alba*, *Carpinus betulus*, *Tilia cordata*, *Acer pseudoplatanus*, *Betula* spp., *Fraxinus excelsior*,  
641 *Quercus* spp., *Alnus glutinosa*, and *Pinus sylvestris*.

642 **1.9.7 Simulations**

643 We simulated forest dynamics from bare ground for each site, using patches (pixels) with a size of 20x20  
644 cm<sup>2</sup>. We prepared landscapes of 250x250 m without topographical variation for each site. The simulations  
645 we run from bare ground to 2000 years, and the samples were taken starting in the year 2000. In the  
646 regeneration module, we used (1) a base seeding probability of 0.001, which defines if seeds are available  
647 due to background seed rain; (2) a dispersal mode based on the formulation ‘random asymmetric’; and (3)  
648 the same establishment probability of 0.9 for all species included in the simulation of, which sets the same  
649 probability for all the species to regenerate successfully, provided that the abiotic and light conditions are  
650 suitable for establishment.

651 **1.9.8 Outputs**

652 We estimated the outputs based on a sample of 25 random cells every ten years from the simulation years  
653 2010 to 4000 for one simulation per site, thus providing the required 200 samples per site.

654 **1.10 Landis II**

655 **1.10.1 Authors**

656 Josef Bruna, Paola Mairotta, Marco Mina, Giorgio Vacchiano

657 **1.10.2 Model**

658 Landscape scale forest simulation model LANDIS-II (Scheller et al. 2007) with PnET-Succession extension  
659 (version 4.1). PnET-Succession is based on the Biomass Succession extension of Scheller and Mladenoff  
660 (2004), embedding elements of the PnET-II ecophysiology model of Aber et al. (1995) to mechanistically  
661 simulate growth as a competition for available light and water (De Bruijn et al. 2014). PnET-Succession  
662 simulates the competition among cohorts for water and light at a monthly time-step as a function of photo-  
663 synthetic processes and maintenance respiration that are explicitly linked to environmental drivers such as  
664 temperature, precipitation, photosynthetic active radiation (PAR), and CO<sub>2</sub> concentration. Regeneration  
665 depends on distance from a seed source, soil water, and subcanopy light, while competition is modeled by  
666 partitioning incoming light through multiple canopy layers. Growth of specific cohort biomass components  
667 is allocated in the following order: non structural carbon, first, then foliage then root and stem. Biomass  
668 growth decreases as cohorts approach their longevity age but mortality can occur at any time when carbon  
669 reserves production is insufficient to support growth due to shading, water competition, and/or drought  
670 (Gustafson et al. 2015), or by any disturbance or management extension used. For output, we selected  
671 Biomass Community Output Extension version 2.0.1, which generates output in the format: species age  
672 biomass (g / m<sup>2</sup>) at specified time steps.

673 The most complete reference resources for the LANDIS-II model and regeneration module are:

- 674 • Scheller R.M. & Mladenoff D.J. (2004) A forest growth and biomass module for a landscape simulation  
675 model, LANDIS: design, validation, and application. Ecological Modelling 180: 211–229. <https://doi.org/10.1016/j.ecolmodel.2004.01.022>

- Scheller, R. M., Domingo J. B. , Sturtevant B. R. , Williams J. S. , Rudy A. , Gustafson E. J. & Mladenoff D. J. (2007) Design, development, and application of LANDIS-II, a spatial landscape simulation model with flexible temporal and spatial resolution. Ecological Modelling 201(3-4): 409–419. <https://doi.org/10.1016/j.ecolmodel.2006.10.009>
- de Bruijn A., Gustafson E.J. , Sturtevant B.R., Foster J.R., Miranda B.R., Lichti N.I. & Jacobs D.F. (2014) Toward more robust projections of forest landscape dynamics under novel environmental conditions: Embedding PnET within LANDIS-II. Ecological Modelling (287): 44–57 <https://doi.org/10.1016/j.ecolmodel.2014.05.004>
- Petter G., Mairotta P., Albrich K., Bebi P., Bruna J., Bugmann H., Haffenden A., Scheller R.M., Schmaltz D.R., Seidl R., Speich M., Vacchiano G. & Lischke H. (2020) How robust are future projections of forest landscape dynamics? Insights from a systematic comparison of four forest landscape models. Environmental Modelling & Software 134: 104844. <https://doi.org/10.1016/j.envsoft.2020.104844> (supplementary material)
- Gustafson E.J., De Bruijn A.M.G., Pangle R.E., Limousin J.M., McDowell N.G., Pockman W.T., Sturtevant B.R., Muss J.D. & Kubiske M.E. (2015) Integrating ecophysiology and forest landscape models to improve projections of drought effects under climate change. Global Change Biology 21: 843–856. <https://doi.org/10.1111/gcb.12713>

### 695 1.10.3 Climate

696 Climate input was generated by randomly selecting entire years from the monthly data from the CHELSA  
 697 dataset and collating them one after the other to create a 2000 years series. The sampling was repeated  
 698 10 times with different random order of years to create the 10 climate replicates. Selecting a year at a  
 699 time eliminates inconsistent seasons (especially summer). We used monthly mean, minimum and maximum  
 700 temperatures and precipitation as input for PnET succession extension. PnET-Succession also requires mean  
 701 monthly values of PAR during daylight hours, which we calculated by dividing the monthly rsds data by  
 702 the number of daylight seconds in each month for latitude 47 to get W/m<sup>2</sup>. We then multiplied this by 4.6  
 703 to get mol/m<sup>2</sup>/s and multiplied by 0.5 to get PAR part of the spectrum, based on the approximation by  
 704 Tsubo et al. (2005). Leap years were not considered. The PAR distribution across all sites and years is in  
 705 range with values that are typical for temperate regions.

706 CO<sub>2</sub> concentration with yearly timestep was added from the concentrations table available from EEA (2019).  
 707 For years 0-1750 CO<sub>2</sub> concentration was maintained fixed to 278 ppm. As for the period 1750-1975 there  
 708 was only one value each 5 years, we used a constant value for each 5-year period. CO<sub>2</sub> concentration was  
 709 added to the climate input file after randomization of temperature, precipitation and PAR (see above), so  
 710 it reflects realistic values for the simulated years. Simulations were run from year 0 to 1990 but sampled  
 711 outputs did not exceed year 1910. Thus, the drastic increase in CO<sub>2</sub> concentration during the second half  
 712 of the 1900s did not affect the delivered results.

### 713 1.10.4 Soil

714 Soil type was set to LOAM at all sites. Rooting depth was calculated from soil quality codes (1-5, original  
 715 values ranged from 1.13 to 4.87) multiplied by 205. This produces a soil depth in the range 231 - 998  
 716 mm, that are within the typical range for PnET-Succession (maximum 1000 mm). A clear trend emerged -  
 717 deeper soils resulted in higher biomass, although with some exceptions.

### 718 1.10.5 Topography

719 The ecoregion-specific parameter Precipitation Loss Fraction denotes the water lost to runoff induced by  
 720 topographic slope. We estimated this parameter for each site from topo\_data\_200 dataset as slope \*  
 721 0.01 (e.g., 12% slope = 0.12 PrecLossFrac). We acknowledge that this is a simplification and that better  
 722 parameterization would be possible if soil types were available for each site. Tests showed that sites with

723 extreme slope tended to have lower biomass, but the signal was not that clear. The correlation between  
724 slope and elevation was 0.6 which could obscure the results.

725 Some sites at very high elevation had, correspondingly, very low temperature. At these sites, the model  
726 showed a visible trend in producing lower biomass (down to zero at a few sites). Yet this was probably  
727 not apparent in the regeneration results, as extremely low biomass could still support regeneration, even if  
728 cohorts do not live long, due to our modification of sexual maturity age.

### 729 1.10.6 Tree species

730 As LANDIS-II cannot start from bare ground, initial communities were set to include all species defined in  
731 the protocol at all sites starting with 10-years old cohorts of the following species: fasy (*Fagus sylvatica*),  
732 pabi (*Picea abies*), abal (*Abies alba*), cabe (*Carpinus betulus*), tico (*Tilia cordata*), acps (*Acer pseudoplatanus*),  
733 betu (*Betula spp.*), frex (*Fraxinus excelsior*), quer (*Quercus spp.*), algl (*Alnus glutinosa*), pisy (*Pinus sylvestris*). The species-specific parameter denoting sexual maturity was set to 10 years equally for all species,  
734 so that seed source of all species is available from the onset of the simulations at all sites and to maintain  
735 seed in the landscape pool. Vegetative regeneration (resprouting) was prevented, since this would have an  
736 effect on allometry and regeneration.

737 Some species may be under or overrepresented because their occurrence in LANDIS-II simulations is typically  
738 due to small-scale disturbances or management which were not included in the simulations.

739 The model requires two sets of parameters representing species-specific life traits. The first set is used by the  
740 LANDIS-II core module. The species-specific parameter denoting “longevity” and “sexual maturity” were  
741 the only parameters of this set considered in the current exercise. The “sexual maturity” was set to 10 years  
742 equally for all species, so that seed source of all species is available from the onset of the simulations at all  
743 sites and to maintain seed in the landscape pool. Vegetative regeneration (resprouting) was prevented since  
744 this would influence allometry and regeneration.

745 The second set is used by the PnET-Succession extension and includes several ecophysiological parameters.  
746 For this second set we started with the values already applied in Petter et al. (2020) with a previous version  
747 of PnET. The values of some of the parameters to which PnET is most sensitive and/or for which the  
748 range of variation had been modified for PnET4.1 were then iteratively adjusted (individually and then  
749 in combination) to meet the requirements of PnET version 4.1 used in this exercise. The changes were  
750 implemented one by one in simulations with the exercise data and those leading to an output deemed  
751 realistic and to a relative stabilization of the biomass trend through the simulation were retained for the  
752 implementation of the full set of replicates. The retained changes include: 1) decreased percentage of foliar  
753 nitrogen for algl (*Alnus glutinosa*); 2) rescaling to the new ranges for all species of the values of the Halfsat  
754 and the FracBelowG. The first of these parameters represents shade tolerance and its value affects the  
755 probability of establishment of a species (Half saturation light level for photosynthesis.); the latter regulates  
756 allocation between above and below ground pool (Fraction of non-foliar biomass that is belowground (root  
757 pool)) ; 3) a slight decrease of the value of the parameter (Fracfol) affecting the yearly allocation to foliage  
758 of the active total woody biomass for the three conifers abal (*Abies alba*), piab (*Picea abies*), pisy (*Pinus*  
759 *sylvestris*).

### 760 1.10.7 Simulation

761 Simulation area was defined as a rectangle of 10×20 dimension with sites (i.e., cells) of 1-ha. Each site is  
762 an individual ecoregion (i.e., one cell - as in our case - or group of cells sharing similar climate and soil  
763 conditions, as a way in LANDIS-II to define differences in biophysical conditions across landscapes) with  
764 specific values for soil quality, topography and climate, based on the data provided. The model runs with a  
765 yearly timestep using monthly climate. We started each model run with initial communities of all species at  
766 age 10 at all sites. Each run was simulated for 1980 years.

768 **1.10.7.1 Dispersal** We have used the non-spatial seeding algorithm “universal dispersal” for all the  
769 model runs. This way, every species can seed any forest site in the landscape (across all the 200 sites). This  
770 mode does not take into account the spatial arrangement and contiguity of cells (i.e., no active seed dispersal),  
771 which is proper for the sake of the model comparison exercise. Yet in real landscape seed limitation can also  
772 play a role in species composition. The seed number is affected by species-specific age of maturity, which we  
773 have modified. This setting ensures an influx of seeds from outside consistent with the original settings.

774 **1.10.7.2 Sampling design** We have sampled each site 20 times along the simulation run in two time  
775 windows starting 50 years after the first cycle following typical species longevity. After the year 700, biomass  
776 of most species was relatively stable and we sampled every 50 years, starting at 750 until the year 1200. The  
777 next sampling period started from 1450 and continued until 1900, i.e., after the next longevity peak, again  
778 every 50 years. At each selected sampling time, we extracted cohorts of each species according to the age  
779 related to the two DBH thresholds (7cm/10cm). Additionally, we extracted cohorts that were up to 9 years  
780 older than these thresholds, to get the expected results for a 10-year interval. For example, *Fagus sylvatica*  
781 reaches DBH 7cm at 17 years, therefore we have selected all cohorts with age 17-26.

782 To deliver more than one simulation per site, we created 10 replicates with different climate replicate and  
783 random number generator seed number to account for stochastic processes in PnET-Succession. This resulted  
784 in the expected 200 samples for each site.

## 785 **1.10.8 Outputs**

786 Sample number code

787 Number (1-200) was defined as sample in time + (replicate-1)\*20, with sample in time (1-20) according to  
788 the sample order. Replicate (1-10) combines random number and climate sequence. For example sample  
789 number 25 was taken from the climate replicate 2 and the fifth sample in time (year 950).

790 r.trees

791 As LANDIS-II outputs are expressed in terms of cohort age and mean biomass per site, we have calculated  
792 the mean DBH and biomass of each species based on age. We estimated the age when each species reaches 7  
793 cm and 10 cm DBH and the number of individuals using allometric models from the Italian forest inventory  
794 collected in R package ForIT (Puletti et al. 2014), and unpublished data from the study by Mina et al. (2021).  
795 Please note that the equations used predict DBH >0 already for a tree with age 1, this is because it is based  
796 on forestry data and tree cores. The real age when reaching 1.3 m height is species specific and we did not  
797 implement this offset. For each cohort, we divided the cohort biomass reported by LANDIS-II, recalculated  
798 to kg/ha by the mean biomass of a tree of the same species and age to obtain the number of trees of each  
799 species per site. We rounded all results up to the nearest integer to avoid any fraction of trees. The number  
800 of individuals was aggregated for all the cohorts of the age of reaching 7 cm or 10 cm DBH and all cohorts  
801 of the same species that were up to 9 years older. This approach does not reflect influence of site conditions  
802 or stand densities on Age-DBH and Age-Biomass. Relationships between age and DBH were derived by  
803 fitting asymptotic regressions using individual tree measurements from an ensemble of forest inventory plots  
804 distributed across south-eastern Canada (see Supporting information of Mina et al. 2021). This was the  
805 only public dataset for which we could relate tree age, derived from stem coring and tree ring analysis, to  
806 measured DBH. Although tree age measurements were obtained with a robust methodology, these functions  
807 do not disentangle the influence of site conditions or stand densities. Additionally, they reflect growing  
808 conditions of tree genera in Eastern North America.

809 r.ba basal area of regeneration Calculated as a sum of r.ba of all the cohorts selected in r.trees using the  
810 following formula: DBH2 \* /4 \* r.tree.

811 ba: total basal area We have not calculated this since our allometric equations do not cover older ages.  
812 Therefore, we produced the following two biomass variables as a surrogate. The basal area was later calcu-  
813 lated as a sum of r.ba and estimated ba based on biomass. The estimation includes transformation of kg  
814 into tonnes / ha and expansion factor 12.5 to transform ba m<sup>2</sup>/ha.

815  $((\text{landis\$sum.bio} - \text{landis\$r.bio.sum}) * 0.001) / 12.5$ ). This includes  
816 sum.bio  
817 Biomass of all cohorts of the species on site including the regeneration and even younger regeneration (units  
818 kg/ha).  
819 r.bio.sum Biomass of the regeneration cohorts corresponding to the r.ba and r.trees on site (units kg/ha).  
820 Please notice that we included 0 values for species missing in a given sample and for samples in sites where  
821 Landis did not simulate any tree.

## 822 1.10.9 References

823 Aber J. D. & Federer C. A. (1992). A generalized, lumped-parameter model of photosynthesis, evapotranspiration and net primary production in temperate and boreal forest ecosystems. *Oecologia* 92(4): 463-474.  
824  
825 Aber J.D., Ollinger S.V., Federer C.A., Reich P.B., Goulden M.L., Kicklighter D.W., Melillo J.M. & Lathrop R.G. Jr. (1995) Predicting the effects of climate change on water yield and forest production in the northeastern United States. *Climate Research* 5(3): 207–22.  
826  
827 de Bruijn A., Gustafson E.J. , Sturtevant B.R., Foster J.R., Miranda B.R., Lichti N.I. & Jacobs D.F. (2014) Toward more robust projections of forest landscape dynamics under novel environmental conditions: Embedding PnET within LANDIS-II. *Ecological Modelling* (287): 44–57  
828  
829 EEA (2019) Trends in atmospheric concentrations of CO<sub>2</sub> (ppm), CH<sub>4</sub> (ppb) and N<sub>2</sub>O (ppb), between 1800 and 2017 available at [https://www.eea.europa.eu/ds\\_resolveuid/217c026ca03649398aadf39d87623e57](https://www.eea.europa.eu/ds_resolveuid/217c026ca03649398aadf39d87623e57)  
830  
831 Gustafson, E. J., A. M. G. De Bruijn, R. E. Pangle, J.-M. Limousin, N. G. McDowell, W. T. Pockman, B. R. Sturtevant, J. D. Muss, and M. E. Kubiske. 2015. Integrating ecophysiology and forest landscape models to improve projections of drought effects under climate change. *Global Change Biology* 21:843–856.  
832  
833 Mina, M., Messier, C., Duveneck, M., Fortin, M. J., & Aquilué, N. 2021. Network analysis can guide resilience-based management in forest landscapes under global change. *Ecological Applications*, 31(1), 1–18.  
834  
835 Petter G., Mairotta P., Albrich K., Bebi P., Brüna J., Bugmann H., Haffenden A., Scheller R.M., Schmatz D.R., Seidl R., Speich M., Vacchiano G. & Lischke H. (2020) How robust are future projections of forest landscape dynamics? Insights from a systematic comparison of four forest landscape models. *Environmental Modelling & Software* 134: 104844. <https://doi.org/10.1016/j.envsoft.2020.104844>  
836  
837 Puletti N., Mura M., Castaldi C., Marchi N., Chiavetta U. and Scotti R. (2014). ForIT: Functions from the 2nd Italian Forest Inventory (INFC). R package version 1.0. <https://CRAN.R-project.org/package=ForIT>  
838  
839 Scheller, R. M., Domingo J. B. , Sturtevant B. R. , Williams J. S. , Rudy A. , Gustafson E. J. & Mladenoff D. J. (2007) Design, development, and application of LANDIS-II, a spatial landscape simulation model with flexible temporal and spatial resolution. *Ecological Modelling* 201(3-4): 409–419. <https://doi.org/10.1016/j.ecolmodel.2006.10.009>  
840  
841 Tsubo M. & Walker S. (2005) Relationships between photosynthetically active radiation and clearness index at Bloemfontein, South Africa. *Theoretical and Applied Climatology* 80: 17–25. <https://doi.org/10.1007/s00704-004-0080-5>

## 851 1.11 TreeMig

### 852 1.11.1 Authors

853 Heike Lischke

854 **1.11.2 Model**

855 The model TreeMig (see treemig.wsl.ch) was originally based on the ForClim model, then aggregated by a  
856 distribution based approach (Lischke et al. 1998), and extended to a forest landscape model by including  
857 seed production, seed dispersal, seed bank dynamics and seedling establishment (Lischke and Loffler 2006,  
858 Lischke et al. 2006).

859 The most complete reference resource for the TreeMig model and regeneration module are:

- 860 • Lischke, H., T. J. Loffler, and A. Fischlin. 1998. Aggregation of individual trees and patches in forest  
861 succession models: Capturing variability with height structured, random, spatial distributions. Theor  
862 Popul Biol 54:213-226.
- 863 • Lischke, H., N. E. Zimmermann, J. Bolliger, S. Rickebusch, and T. J. Loffler. 2006. TreeMig: A forest-  
864 landscape model for simulating spatio-temporal patterns from stand to landscape scale. Ecological  
865 Modelling 199:409-420.
- 866 • Lischke, H., and T. J. Loffler. 2006. Intra-specific density dependence is required to maintain species  
867 diversity in spatio-temporal forest simulations with reproduction. Ecological Modelling 198:341-361.
- 868 • The online resources available at treemig.wsl.ch

869 **1.11.3 Climate**

870 As climatic input, the monthly time series of mean temperature and precipitation sum were used. With  
871 these climatic variables and additional data about slope, aspect and soil field capacity, yearly time series of  
872 the following bioclimatic variables were calculated: (1) DDSum, the yearly day degree sum above 5.5°C , (2)  
873 MinWiT, the lowest mean monthly temperature, (3) DrStr, drought stress according to a bucket model that  
874 estimates a monthly PET following (Thorntwaite and Mather 1957), using temperature, latitude, slope and  
875 aspect as input, and calculates the monthly soil water content based on soil water content in the previous  
876 month, precipitation, interception, and field capacity (“bucketsize”) (Bugmann 1994, Fischlin et al. 1995).  
877 Drought stress is then given by 1- the ratio between demand (PET-interception) and the supply, a function of  
878 the soil water content. To get climate data also for the spin-up, bioclimate was calculated from the monthly  
879 data as given, and then extended by sampling from the given data from the end of the climate data to get  
880 1000 years. The same sequence of sampling years was used in all simulations and sites.

881 **1.11.4 Soil**

882 The soil bucketsize (available water capacity of the upmost 1m soil layer) required for the drought stress  
883 calculation, was derived from the soil quality data set, by Bucketsize = 10 + (soil\_quality-1) /4 \* 25 , to  
884 covert the range from 10 cm to 35cm

885 **1.11.5 Topography**

886 Slope and aspect were taken from the topographic data set and converted to a common variable entering  
887 the PET calculation, by slasp=  $2\cos(\text{aspect} \pi/180) * \min(1, \text{slope}/60)$

888 **1.11.6 Tree species**

889 Thirty Central European tree species were simulated, including the standard species of the project . Only  
890 Betula pubescens was not simulated, because we did not have a parametrization for this species at hand.  
891 Species: Abies alba, Larix decidua, Picea abies, Pinus cembra, Pinus montana, Pinus sylvestris, Taxus  
892 baccata, Acer campestre, Acer platanoides, Acer pseudoplatanus, Alnus glutinosa, Alnus incana, Alnus

893 viridis, Betula pendula, Carpinus betulus, Castanea sativa, Corylus avellana, Fagus sylvatica, Fraxinus  
894 excelsior, Populus nigra, Populus tremula, Quercus petraea, Quercus pubescens, Quercus robur, Salix alba,  
895 Sorbus aria, Sorbus aucuparia, Tilia cordata, Tilia platyphyllos, Ulmus glabra

896 **1.11.7 Simulation**

897 The simulations were carried out on a grid of 15 x 15 cells, each with 200 m side length.

898 **1.11.7.1 Dispersal** The seeds produced by the mother trees are transported from the source cell accord-  
899 ing to a double negative exponential, species specific that determines the share of the seeds in the source cell  
900 landing in a sink cell in a given distance to the source cell. In the sink cells, the seeds enter the seed bank  
901 . At the start of the simulation for 10 years seeds of all species are available in all grid cells, from then on,  
902 the normal seed dispersal starts.

903 **1.11.7.2 Regeneration processes** TreeMig simulates the full feedback from seed production to in-  
904 growth. Some of the involved processes depend on environment. (1) Overall seed production in TreeMig  
905 is described by multiplying a species specific seed production per tree that depends on tree size and thus  
906 indirectly on the growth, which depends on DDsum, drought stress, nutrients and light and the adult tree  
907 number that depends on survival that depends on DDsum, drought stress, nutrients and light. (2) Seed  
908 dispersal is independent of environment. (3) Seed bank dynamics – also environment independent - is given  
909 by seed input, seed mortality, and germination. Additionally, the number of seeds S of a species in the seed  
910 bank of this species (SB) is limited to a carrying capacity C of 1000, by  
911 
$$SB = C + (SB - C) * Exp(-S/C).$$

912 (4) Germination and seedling survival depend on browsing, drought, winter temperature, DDSum and light.  
913 (5) The saplings up to 1.37 die and grow like adult trees, depending on DDsum, drought stress and light.  
914 Only the parameter value of the light dependence differs from that of the adult trees.  
915 The regeneration processes were simulated annually in the order 1. germination, 2. germinated seeds leave  
916 the seed bank, 3. mortality of seeds in the seed bank, 4. seed entry by seed dispersal. The ingrowth numbers  
917 were very sensitive to this order. Simulations with another sequence, in which the seeds in the seed bank  
918 died first and then the remaining ones germinated, resulted in about half the ingrowth.

919 **1.11.7.3 Simulation length** The simulations were started on bare ground and run for 1000 years, when  
920 at all sites the equilibrium was reached.

921 **1.11.7.4 More simulations per site** TreeMig simulates directly the mean dynamics of entire stands,  
922 but based on the variability of light conditions within the stand [distribution based approach, Lischke, 1998,  
923 aggregation. To come up with the required 200 random patches of 1 ha, temporal and spatial variability  
924 intrinsic to TreeMig were combined. Temporal variability was given by sampling from each decade of the  
925 last 100 years of the simulation, i.e. years 900-1000. For each of these 10 decades, 20 grid cells were sampled  
926 from the simulated grid, reflecting spatial variability, results from demographic stochasticity and short-range  
927 spatial interactions

928 **1.11.8 Outputs**

929 In contrast to gap models, TreeMig is based on the concept of frequency distributions of tree densities classes  
930 in different tree heights on ca. 1/12 ha ( $833\text{m}^2$ ) patches, and the resulting frequency distributions in discrete  
931 light. During the simulation, in each height class the frequencies of the different light classes were recorded,  
932 as well as the ingrowth of each species in the height-light class. By sampling 12 times from the height-light  
933 class ingrowths according to the height-light class frequency distribution and summing up, the stochastic  
934 ingrowths into all TreeMig height classes for one ha were calculated for each grid cell. Then the height class

935 boundaries were translated into DBH and the ingrowths into the height classes linearly interpolated to 7cm  
936 and 10cm. The ingrowth basal areas into the height classes were obtained by multiplying the interpolated  
937 ingrowth numbers with the basal areas at 7cm and 10cm, i.e. r.trees \* Pi\* (0.07/2)2 and r.trees \* Pi\* (0.1/2)2  
938 . The species specific basal area (at 1.37m) sums are a standard output of TreeMig, given by multiplying  
939 the state variables (number of trees per grid cell, height class, and species) with the species specific basal  
940 area of each height class. To account for the ingrown trees dying within a decade, as an approximation the  
941 survival in each year to the power of 5 was used. Thereby, it was assumed that the trees have to survive in  
942 average 5 years in each decade, and that the current mortality is valid for these 5 years.

#### 943 1.11.9 References

- 944 Bugmann, H. 1994. On the ecology of mountainous forests in a changing climate: A simulation study.  
945 Dissertation. Swiss Federal Institute of Technology, Zurich.
- 946 Fischlin, A., H. Bugmann, and D. Gyalistras. 1995. Sensitivity of a forest ecosystem model to climate  
947 parametrization schemes. Env. Poll. 87:267-282.
- 948 Lischke, H., and T. J. Loffler. 2006. Intra-specific density dependence is required to maintain species diversity  
949 in spatio-temporal forest simulations with reproduction. Ecological Modelling 198:341-361.
- 950 Lischke, H., T. J. Loffler, and A. Fischlin. 1998. Aggregation of individual trees and patches in forest  
951 succession models: Capturing variability with height structured, random, spatial distributions. Theor Popul  
952 Biol 54:213-226.
- 953 Lischke, H., N. E. Zimmermann, J. Bolliger, S. Riekebusch, and T. J. Loffler. 2006. TreeMig: A forest-  
954 landscape model for simulating spatio-temporal patterns from stand to landscape scale. Ecological Modelling  
955 199:409-420.
- 956 Thornthwaite, C. W., and J. R. Mather. 1957. The water balance. Publications in Climatology VIII:1-69.

## 957 1.12 LPJ-GUESS

### 958 1.12.1 Authors

959 Tim Anders, Jessica Hetzer, Thomas Hickler

### 960 1.12.2 Model

961 The model was originally developed by Ben Smith of Lund University in a collaboration also involving the  
962 Potsdam Institute for Climate Impact Research and the Max-Planck Institute for Biogeochemistry. Over  
963 the years, many people from institutes around the world have contributed to the refinement and further  
964 development of the model.

965 We used the process-based mechanistic model LPJ-GUESS to simulate vegetation dynamics considering tree  
966 species, age cohorts, gap dynamics and biogeochemical cycles. Parameters of the model reflect an updated  
967 version of the most common European tree species as well as typical shrub PFTs as described by Hickler et  
968 al. (2012).

969 The most complete reference resource for the LPJ-GUESS model and regeneration module is:

- 970 • Smith, B. (2001). LPJ-GUESS-an ecosystem modelling framework. Department of Physical Geography  
971 and Ecosystems Analysis, INES, Sölvsgatan, 12, 22362.
- 972 • Smith, B., Wårlind, D., Arneth, A., Hickler, T., Leadley, P., Siltberg, J., & Zaehle, S. (2014). Im-  
973 plications of incorporating N cycling and N limitations on primary production in an individual-based  
974 dynamic vegetation model. Biogeosciences, 11(7), 2027-2054.
- 975 • Source code is available on demand (see <https://web.nateko.lu.se/lpj-guess/>).

976 **1.12.3 Climate**

977 We used the provided daily time series of climatic variables from 1981 to 2018. The climatic variables base  
978 on the CHELSA data set with a spatial resolution of  $0.008^\circ \times 0.008^\circ$  ( $\sim 1$  km) (Karger et al., 2021). Daily  
979 average temperature (tas) [ $^\circ\text{C}$ ], daily average maximum temperature (tasmax) [ $^\circ\text{C}$ ], daily average minimum  
980 temperature (tasmin) [ $^\circ\text{C}$ ], precipitation sum (pr) [mm] and surface solar (shortwave) radiation (rsds) were  
981 taken to set up the LPJ-GUESS simulation. Used climatic variables were converted to netCDF files. As  
982 LPJ-GUESS requires the climatic variables in specific units, temperature variables (tas, tasmax, tasmin) [ $^\circ\text{C}$ ]  
983 were converted to Kelvin and surface solar radiation (rsds) [ $\text{Jm}^{-2}$ ] was converted to  $\text{W/m}^2$  by dividing rsds  
984 by  $86400$  s ( $3600$  s/h \*  $24$  h). Nitrogen deposition was considered to be constant at a level of  $10 \text{ kgN/ha/year}$ .  
985 Atmospheric carbon dioxide concentration data from 1900 to 2018 was taken from the global carbon project  
986 (Quéré et al. 2018).

987 **1.12.4 Soil**

988 All sites were simulated with default values for a medium textured soil type (sand: 0.35, clay: 0.15, 823 silt:  
989 0.5) in LPJ-GUESS.

990 **1.12.5 Topography**

991 Topography was not considered.

992 **1.12.6 Tree species**

993 LPJ-GUESS can be run in different modes, with different levels of abstraction of the population and com-  
994 munity processes. For this study, the more detailed ‘cohort’ mode was used, in which individuals, patches  
995 and vertical canopy structure are represented explicitly, but living individuals within a cohort (age class)  
996 of a given tree species in a given patch are assumed to be identical (in terms of all state variables, such as  
997 height and stem diameter). Simulations consider the main tree species as well as other PFTs yielding an  
998 appropriate representation of European vegetation, including only tree and shrub species that are widely  
999 distributed across Europe and can become dominant in some areas (Hickler et al., 2012). Mediterranean  
1000 rain-green small shrubs with shallow roots (e.g. *Lavendula* spp., *Rosmarinus* spp.) and alpine/arctic shrubs  
1001 (e.g. *Vaccinium* spp.) were represented as PFTs in the model. As in earlier applications of LPJ-GUESS,  
1002 herbaceous vegetation was represented by two ‘generic herb’ PFTs, with C3 and C4 photosynthesis, respec-  
1003 tively. The final set included 16 tree species, one Mediterranean shrub PFT, one boreal/alpine shrub PFT,  
1004 and the two herbaceous PFTs described earlier (Table 2). To increase the chances of shade-intolerant species  
1005 becoming established, patch-destroying disturbances were allowed as described in Hickler et al. 2012. *Acer*  
1006 *pseudoplatanus* and *Alnus glutinosa* are not parameterized in LPJ-GUESS and therefore not considered.

1007 **1.12.7 Simulation**

1008 In this study, vegetation is simulated in so called patches that represent forest areas of fixed size. Patches  
1009 can be regarded as sample stands in a grid cell, each of which represents an  $0.1 \text{ ha}$  (comparable to figure  
1010 1 of the tree regeneration workshop protocol). In this study, vegetation dynamics were simulated by 2000  
1011 replicate patches each  $0.1 \text{ ha}$  in size. To match the required sample size, we processed the data so that ten  
1012  $0.1 \text{ ha}$  patches were merged to one  $1 \text{ ha}$  sample.

1013 **1.12.7.1 Dispersal** Model formulations of establishment are based on those employed within the ‘forest  
1014 gap’ model FORSKA (Leemans & Prentice, 1989; Prentice et al., 1993). The number of new saplings of each  
1015 woody PFT/species and in each patch each year is drawn at random from the Poisson distribution, with an  
1016 expectation influenced by a PFT/species-specific maximum establishment rate and by the ‘propagule pool’,

1017 i.e. the amount of carbon allocated to reproduction by all individuals of the PFT/species at all patches in  
1018 the previous year. No saplings are established in a given patch if the minimum PAR level at the forest floor  
1019 is below a PFT/species-specific threshold, which is higher for more light-demanding PFTs/species.

1020 **1.12.7.2 Simulation length** What is the simulation length, and how have you determined the simulation  
1021 time until the equilibrium?

1022 The simulations were initialized from bare ground (no biomass) and the model was spun up for 500 years  
1023 until the modelled vegetation was in approximate equilibrium with the climate and CO<sub>2</sub> around the year  
1024 1900 (Smith et al., 2001; Hickler et al., 2012).

1025 If you have run more than one simulation per site, please describe the differences of the approaches used.  
1026 We performed one simulation per site.

## 1027 **1.12.8 Output**

1028 The generated output file is called Output\_SGN\_LPJGUESS.txt. Each row of the output dataset contains  
1029 variables regarding the decade 2008-2018. The first two columns describe the study site (column “site”, val-  
1030 ues reflect site ID) and the 1 ha samples of that specific site (column “sample”, values range from 1 to 200).  
1031 Output variables are species-specific. Although we simulated a total of 20 European tree species and PFTs,  
1032 our output file considers only the species required by the protocol (column “species”, values are the abbrevi-  
1033 ations for the species name (“abal” for Abies alba, “cabe” for Carpinus betulus, “fasy” for Fagus sylvatica,  
1034 “frex” for Fraxinus excelsior, “pabi” for Picea abies, “pisy” for Pinus sylvestris , “tico” for Tilia cordata ,  
1035 “betu\_pen” for Betula pendula, “betu\_pubescens” for Betula pubescens, “quer\_il” for Quercus ilex, “quer\_pub”  
1036 for Quercus pubescens, and “quer\_rob” for Quercus robur). Since Acer pseudoplatanus (“acps”) and Alnus  
1037 glutinosa (“algl”) are not parameterized for LPJ-GUESS so far, we have not included these species in the  
1038 output. Further we excluded shrubs (alpine/arctic shrubs and Quercus coccifera) and herbaceous vegetation  
1039 from the final output as this study focusses on tree regeneration only. The first variable is the number of 7  
1040 cm recruits “r\_7cm.trees” calculated as the sum of all trees of the same species that cross the threshold of  
1041 7 cm DBH between 2008 and 2018 in that specific sample of that specific site. The variable “r\_10cm.trees”  
1042 refers to 10 cm threshold respectively. The 7 cm recruits’ basal area „r\_7cm.ba” is calculated as a weighted  
1043 sum of r\_7cm.trees multiplied by recruits basal area at that time (with ba=(dbh/2) ). Similarly, r\_10cm.ba  
1044 was calculated for 10 cm recruits. The last two columns describes the mean annual basal area and the mean  
1045 number of trees per site, sample, and species overall years between 2008 and 2018 (column “ba”).

1046 Table 1: Species/PFT characteristics and parameter of Hickler et al. 2012. r base respiration rate, kallm1  
1047 constant in allometry equations, Tc,min minimum winter temperature for establishment, Tc,max maximum  
1048 coldest-month temperature for establishment, GDD5 minimum degree-day sum above 5 °C for establishment,  
1049 fAWC minimum growing-season fraction of available soil water holding capacity in the first soil layer, rfire  
1050 fraction of individuals surviving fire, kla:sa leaf longevity, CAmax maximum woody crown area. Parameter  
1051 that are associated with establishment processes are marked in bold. Species/PFT

Species/PFT	Short name	Geographic range	$r^{\wedge}$ (gCgN-'day')	Growth form	$k_{\text{allow}}^{\wedge}$ ("C)	$T_{c,\min}^{\wedge}$ ("C)	$T_{c,\max}^{\wedge}$ ("C)	$GDD_0^{\wedge}$ ("Cd)	fAWC	Chilling requirement <sup>a</sup>	Shade tolerance class	$r_{\text{fro}}$	$k_{\text{allow}}^{\wedge}$ ("yr)	$Z_{t^{++}}$ ("yr)	$a_{\text{leaf}}^{\wedge}$ ("yr)	$a_{\text{ind}}^{\wedge}$ ("m <sup>2</sup> )	$CA_{\max}^{\wedge}$
<i>Abies alba</i>	abal	temperate	0,055	tree	150	-4,5	-2	1450	0,35	-	tolerant	0,1	4000	0,8	4	350	40
<i>Betula pendula</i>	betu_pen	temperate	0,055	tree	250	-30	-	700	0,42	intermediate	intolerant	0,1	5000	0,8	0,5	200	40
<i>Betula pubescens</i>	betu_pub	boreal	0,11	tree	250	-	-	350	0,5	intermediate	intolerant	0,1	5000	0,8	0,5	200	40
<i>Carpinus betulus</i>	cabe	temperate	0,055	tree	250	-8	-	1200	0,33	high <sup>ab</sup>	intermediate	0,1	5000	0,7	0,5	350	40
<i>Corylus avellana</i>	cor_ave	temperate	0,055	tree	250	-8	-	800	0,3	intermediate	intolerant	0,1	4000	0,7	0,5	300	15
<i>Fagus sylvatica</i>	fasy	temperate	0,055	tree	250	-3,5	-	1500	0,3	high <sup>ab</sup>	tolerant	0,1	5000	0,8	0,5	500	40
<i>Fraxinus excelsior</i>	frex	temperate	0,055	tree	250	-16	-	1100	0,4	low	intermediate	0,1	5000	0,8	0,5	350	40
<i>Juniperus oxycedrus</i>	jun_oxy	Mediterranean	0,055	shrub	150	0	-	2200	0,01	-	intolerant	0,4	1500	0,5	1,5	200	10
<i>Picea abies</i>	pabi	boreal	0,11	tree	150	-30	-1,5	600	0,43	-	tolerant	0,1	4000	0,8	4	500	40
<i>Pinus halepensis</i>	pin_hal	Mediterranean	0,055	tree	150	3	-	3000	0,05	-	intolerant	0,4	2000	0,6	2	350	40
<i>Pinus sylvestris</i>	pisy	boreal	0,11	tree	150	-30	-1	500	0,25	-	intermediate	0,4	2000	0,6	2	500	40
<i>Quercus coccifera</i>	quer_coc	Mediterranean	0,055	shrub	250	0	-	2200	0,1	-	intermediate	0,3	2500	0,5	1,5	350	10
<i>Quercus ilex</i>	quer_il	Mediterranean	0,055	tree	250	-2	-	1800	0,1	-	intermediate	0,3	3000	0,5	2	350	40
<i>Quercus pubescens</i>	quer_pub	supra-Mediterranean	0,055	tree	250	-5	-	1900	0,2	low	intermediate	0,2	4000	0,6	0,5	500	40
<i>Quercus robur</i>	quer_rob	temperate	0,055	tree	250	-16	-	1100	0,25	low	intermediate	0,2	4000	0,6	0,5	500	40
<i>Tilia cordata</i>	tico	temperate	0,055	tree	250	-18	-	1000	0,33	high <sup>ab</sup>	intermediate	0,1	5000	0,8	0,5	350	40
Boreal evergreen shrub <sup>e</sup>	BES	boreal	0,11	shrub	250	-	-1	300	0,25	-	intolerant	0,1	500	0,8	2	50	3
Mediterranean raingreen shrub <sup>e</sup>	MRS	Mediterranean	0,055	shrub	250	0	-	2200	0,01	low	intolerant	0,3	1500	0,9	1	100	10
C <sub>3</sub> herbaceous		temperate-boreal	0,055	herbaceous	-	-	-	-	0,01	-	-	0,5	-	0,9	1	-	-
C <sub>4</sub> herbaceous		tropical	0,011	herbaceous	-	15,5	-	-	0,01	-	-	0,5	-	0,9	1	-	-

### 1.12.9 References

- Hickler, T., Vohland, K., Feehan, J., Miller, P. A., Smith, B., Costa, L., ... & Sykes, M. T. (2012). Projecting the future distribution of European potential natural vegetation zones with a generalized, tree species-based dynamic vegetation model. *Global Ecology and Biogeography*, 21(1), 50-63.
- Karger, D. N., Lange, S., Hari, C., Reyer, C. P., & Zimmermann, N. E. (2021). CHELSA-W5E5 v1. 1: W5E5 v1. 0 downscaled with CHELSA v2. 0.
- Leemans, R., & Prentice, I. C. (1989). FORSKA-a general forest succession model. *Meddelanden Från Växtbiologiska Institutionen*.Prentice et al., 1993
- Quéré, C., Andrew, R. M., Friedlingstein, P., Sitch, S., Hauck, J., Pongratz, J., ... & Zheng, B. (2018). Global carbon budget 2018. *Earth System Science Data*.
- Smith, B. (2001). LPJ-GUESS-an ecosystem modelling framework. Department of Physical Geography and Ecosystems Analysis, INES, Sölvveganatan, 12, 22362.
- Smith, B., Wårldin, D., Arneth, A., Hickler, T., Leadley, P., Siltberg, J., & Zaehle, S. (2014). Implications of incorporating N cycling and N limitations on primary production in an individual-based dynamic vegetation model. *Biogeosciences*, 11(7), 2027-2054.

### 1.13 aDGVM2

#### 1.13.1 Authors

- Simon Scheiter Senckenberg Biodiversity and Climate Research Centre, Senckenbergsanlage 25, 60325 Frankfurt am Main, Germany

1072 **1.13.2 Model**

1073 We used aDGVM2, an individual-based dynamic vegetation model that is based on concepts from community  
1074 assembly theory and uses a functional trait approach (Langan et al., 2017; Scheiter et al., 2013). The model  
1075 simulates growth, reproduction, and mortality of individual plants while keeping track of state variables,  
1076 such as biomass, height, and leaf area. Each plant in aDGVM2 is characterized by a plant-specific set of  
1077 trait values. Traits describe growth form, leaf characteristics, hydraulic characteristics, resource allocation,  
1078 architecture, reproduction, mortality, and response to disturbance. Most plant traits are linked by trade-offs  
1079 to constrain possible trait combinations. Selection and trait inheritance assemble plant communities that  
1080 are adapted to biotic and abiotic conditions. Plants with trait combinations that allow sufficient growth and  
1081 reproduction rates, and that allow plants to cope with competition and disturbances can contribute their  
1082 trait values to the community trait pool. Trait mutation and recombination may alter trait values in the  
1083 community trait pool. Randomly drawn seeds from the trait pool are added to the plant population and  
1084 new plants start growing from seeds. Plants that are not adapted to the prevailing disturbance regimes,  
1085 biotic and abiotic conditions, or that do not allocate enough carbon to reproduction disappear from the  
1086 population. Therefore, successful ecological strategies emerge dynamically from these community assembly  
1087 and reproduction process. Due to the trait-based approach, species or plant functional types (PFTs) are not  
1088 pre-defined and hard-coded in aDGVM2. Rather, different PFTs or ecological strategies that are adjusted  
1089 to the prevailing biotic and abiotic conditions emerge from community assembly processes (Scheiter et al.,  
1090 2013), and plants can be classified into PFTs or ecological strategies based on their trait values in a post-  
1091 processing step. The aDGVM2 has primarily been developed for tropical and sub-tropical ecosystems and it  
1092 has not been tested and benchmarked for Europe. We applied the model in the original version. Data-model  
1093 comparisons with model results were not done and the model was not changed to improve agreement with  
1094 any data for Europe.

1095 The most complete reference resource for the aDGVM2 model and regeneration module is:

- 1096 • Scheiter S, Langan L, Higgins SI (2013) Next generation dynamic global vegetation models: learning  
1097 from community ecology. NEW PHYTOLOGIST, 198, 957-969.

1098 **1.13.3 Climate**

1099 The aDGVM2 simulates vegetation at daily temporal resolution. We therefore used daily climate input data  
1100 for the period 1981-2018 according to the modeling protocol.

1101 **1.13.4 Soil**

1102 Soil quality data was converted to maximum rooting depth. Specifically, the soil quality value multiplied  
1103 by 2 and the result was used as maximum rooting depth. We used the multiplication, as we typically use  
1104 maximum soil depth and maximum rooting depth of 10m. Previous model simulations showed that rooting  
1105 depth and soil dept have strong impacts on vegetation dynamics by influencing water availability to plants  
1106 (Langan et al., 2017). We therefore considered it as adequate representation of soil quality. Other soil  
1107 characteristics including volumetric water-holding capacity, soil hydraulic conductivity, soil bulk density,  
1108 soil depth, soil texture, soil carbon content, soil wilting point and field capacity were taken from the FAO  
1109 (<http://www.fao.org>, Nachtergaele et al., 2009).

1110 **1.13.5 Topography**

1111 We used elevation according to the modeling protocol. In aDGVM2, elevation is used to calculate atmospheric  
1112 pressure which in turn influences ecophysiological processes related to water and carbon fluxes at leaf and  
1113 canopy level. Information on slope and aspect was not used, as related processes (e.g., impacts on runoff or  
1114 radiation balance) are not implemented in aDGVM2.

1115 **1.13.6 Tree species**

1116 The aDGVM2 does not simulate pre-defined species or PFTs. The 11 tree species included in the mod-  
1117 eling protocol cannot be implemented and parametrized with reasonable effort. We therefore classified  
1118 simulated trees into different ecological strategies as a post-processing step. We used all combinations of  
1119 evergreen/deciduous, light/water triggered phenology, low/high SLA. Evergreen/deciduous phenology and  
1120 light/water triggered phenology are traits implemented in aDGVM2. The threshold to distinguish high and  
1121 low SLA was defined as 20 m<sup>2</sup>/kg. We used these traits as previous simulation experiments showed that  
1122 patterns of these traits emerge along environmental gradients while patterns of other traits implemented in  
1123 aDGVM2 are often less clear. Ecological strategies considered are: low SLA, deciduous, rain-triggered; low  
1124 SLA, deciduous, light-triggered; low SLA, evergreen, rain-triggered; low SLA, evergreen, light-triggered; high  
1125 SLA, deciduous, rain-triggered; high SLA, deciduous, light-triggered; high SLA, evergreen, rain-triggered;  
1126 high SLA, evergreen, light-triggered.

1127 **1.13.7 Simulations**

1128 Simulations followed the modeling protocol. Simulations were conducted for all sites using the provided daily  
1129 climate and soil data. By default, aDGVM2 simulates 1ha stands. To implement the modeling protocol,  
1130 adjustments to scale model results to 1 ha level were therefore not required. The model was initialized by  
1131 default initialization routines, i.e., traits of individual plants were drawn randomly from a pre-defined range  
1132 of values for each trait. Ranges of trait values are provided in Langan et al. (2017). The model was initialized  
1133 with bare ground and 2880 tree seedlings with 100g each. The aDGVM2 simulates both trees and grasses.  
1134 As the simulation experiment aims at tree/forest regeneration, simulations were conducted only with trees  
1135 while grasses were removed.

1136 We conducted 5 replicates for each of the 200 sites to account for stochastic processes in aDGVM2. Stochastic  
1137 processes include random initialization of trait values of initial plant populations, demographic processes  
1138 such as plant mortality or selection of seeds from seed bank, or the community assembly processes including  
1139 mutation and cross-over. Climate time series used for different replicates were identical such that variation  
1140 between replicates can be attributed by stochastic processes in aDGVM2.

1141 Although aDGVM2 includes routines to simulate fire, simulations were conducted in the absence of fire.  
1142 Management was not simulated.

1143 **1.13.8 Dispersal**

1144 The aDGVM2 does not simulate seed dispersal.

1145 **1.13.9 Simulation length**

1146 We first conducted a 600-year spin-up with a randomized order of years 1981-2018 provided in the CHELSA  
1147 daily climate data. Spin-up is required to ensure that both state variables such as biomass and tree cover  
1148 and community trait composition have stabilized and are in a dynamic equilibrium with climate. Previous  
1149 model simulations showed that a 600-year spin-up is sufficient to reach such an equilibrium state (Langan et  
1150 al., 2017). Following the spin-up, we simulated transient vegetation dynamics with daily CHELSA climate  
1151 data for the period 1981-2018.

1152 **1.13.10 Outputs**

1153 To create output variables, we randomly selected 10-year periods within the transient phase (i.e., period 1981-  
1154 2018 after spin-up phase) and calculated averages of all required output variables following the modeling  
1155 protocol. The selected 10-year periods differed between sites and replicates.

1156 The aDGVM2 does not simulate pre-defined species or PFTs and trees were classified into different ecological  
1157 strategies (see section Tree species). Codes for the ecological strategies in the species column of the output  
1158 files are: 1 - low SLA, deciduous, rain-triggered 2 - low SLA, deciduous, light-triggered 3 - low SLA, evergreen,  
1159 rain-triggered 4 - low SLA, evergreen, light-triggered 5 - high SLA, deciduous, rain-triggered 6 - high SLA,  
1160 deciduous, light-triggered 7 - high SLA, evergreen, rain-triggered 8 - high SLA, evergreen, light-triggered  
1161 Simulations were conducted for all 200 sites. We conducted 5 replicates per site to account for stochastic  
1162 processes in aDGVM. In the output files, replicates are given as follows: Replicate 1 – sample 1:200 Replicate  
1163 2 – sample 201:400 Replicate 3 – sample 401:600 Replicate 4 – sample 601:800 Replicate 5 – sample 801:1000

1164 **1.13.11 References**

- 1165 Langan L; Higgins SI; Scheiter S (2017) Climate-biomes, pedo-biomes or pyro-biomes: which world view  
1166 explains the tropical forest - savanna boundary in South America? JOURNAL OF BIOGEOGRAPHY, 44,  
1167 2319-2330.
- 1168 Nachtergaele, F., van Velthuizen, H., Verelst, L., Batjes, N., Dijk- shoorn, K., Van Engelen, V., Fischer, G.,  
1169 Jones, A., Montanarella, L., and Petri, M.: Harmonized world soil database (version 1.1), FAO, Rome, Italy,  
1170 IIASA, Laxenburg, Austria, 2009.
- 1171 Scheiter S, Langan L, Higgins SI (2013) Next generation dynamic global vegetation models: learning from  
1172 community ecology. NEW PHYTOLOGIST, 198, 957-969.

<sup>1173</sup> **2 Supplementary Material 2: Supplementary figures and tables**

<sup>1174</sup> **2.1 Ingrowth levels, tree diversity and mortality in tree establishment**

Table S1: Number of total samples, samples with zero recruitment and the proportion of zero recruitment per model and observed data.

Model	Total (7 cm)	Total (10cm)	No recruitment (7 cm)	No recruitment (10cm)	Percentage of no recruitment (7 cm)	Percentage of no recruitment (10 cm)
Observed	5676	6564	203	238	3.63	3.58
4C	133000	165000	23898	30177	18.29	17.97
ForCEEPS	363000	440000	1	137	0.03	0.00
ForCEEPS(f)	363000	440000	42	202	0.05	0.01
FORMIND	363000	440000	8663	10082	2.29	2.39
ForClim 1	396000	480000	7	28	0.01	0.00
ForClim 11	396000	480000	77	192	0.04	0.02
SIBYLA	363000	440000	1565	5539	1.26	0.43
xComp	297000	360000	0	0	0.00	0.00
PICUS	363000	440000	400	400	0.09	0.11
iLand	363000	440000	26	143	0.03	0.01
LandClim	363000	440000	378	1347	0.31	0.10
Landis II	363000	440000	28621	34844	7.92	7.88
TreeMig	396000	480000	0	0	0.00	0.00
LPJ-GUESS	328000	398000	6742	7140	1.79	2.06
aDGVM2	6600	8000	603	824	10.30	9.14

Table S2: Test of the significance of the differences of Shannon index in each model for 7 and 10 cm threshold.

model	.y.	group1	group2	p	p.adj	p.format	p.signif	method
Observed	ShannonIndexRecruit	7	10	0.5752324	1.0e+00	0.5752300	ns	T-test
4C	ShannonIndexRecruit	7	10	0.0112379	7.9e-02	0.0112400	*	T-test
ForCEEPS	ShannonIndexRecruit	7	10	0.0022439	2.0e-02	0.0022400	**	T-test
ForCEEPS(f)	ShannonIndexRecruit	7	10	0.0001502	1.8e-03	0.0001500	***	T-test
FORMIND	ShannonIndexRecruit	7	10	0.0018175	1.9e-02	0.0018200	**	T-test
ForClim 1	ShannonIndexRecruit	7	10	0.0000000	2.0e-07	0.0000000	****	T-test
ForClim 11	ShannonIndexRecruit	7	10	0.0000078	1.0e-04	0.0000078	****	T-test
SIBYLA	ShannonIndexRecruit	7	10	0.0017112	1.9e-02	0.0017100	**	T-test
xComp	ShannonIndexRecruit	7	10	0.0089858	7.2e-02	0.0089900	**	T-test
PICUS	ShannonIndexRecruit	7	10	0.0343325	2.1e-01	0.0343300	*	T-test
iLand	ShannonIndexRecruit	7	10	0.0539118	2.7e-01	0.0539100	ns	T-test
LandClim	ShannonIndexRecruit	7	10	0.0000000	0.0e+00	0.0000000	****	T-test
Landis II	ShannonIndexRecruit	7	10	0.3486993	1.0e+00	0.3487000	ns	T-test
TreeMig	ShannonIndexRecruit	7	10	0.4182782	1.0e+00	0.4182800	ns	T-test
LPJ-GUESS	ShannonIndexRecruit	7	10	0.8213248	1.0e+00	0.8213200	ns	T-test

## 7 cm diameter threshold

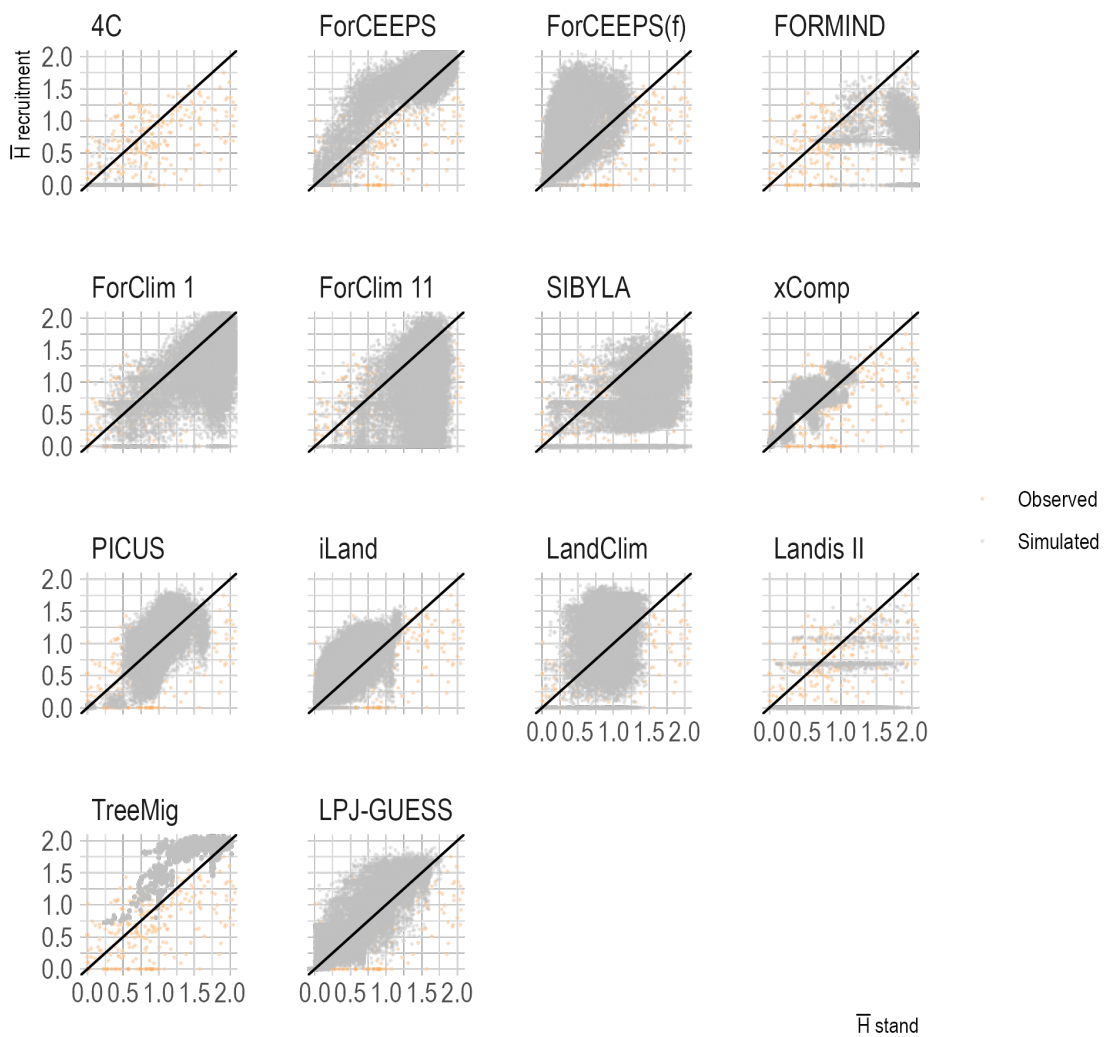


Figure S1: Mean Shannon index per site at recruitment and at the stand level both for observed and simulated values for the diameter threshold of 7cm

## 10 cm diameter threshold

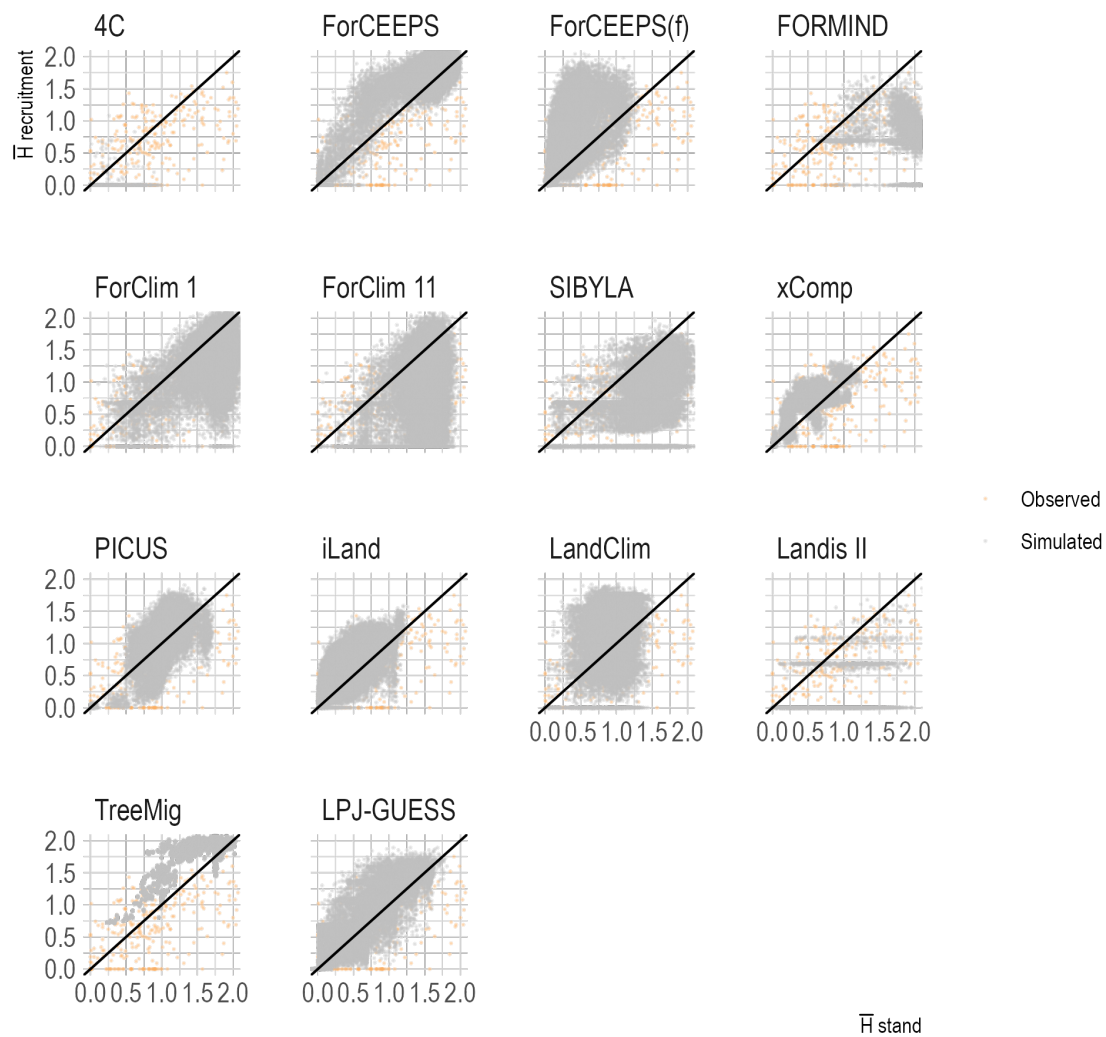


Figure S2: Mean Shannon index per site at recruitment and at the stand level both for observed and simulated values for the diameter threshold of 10cm

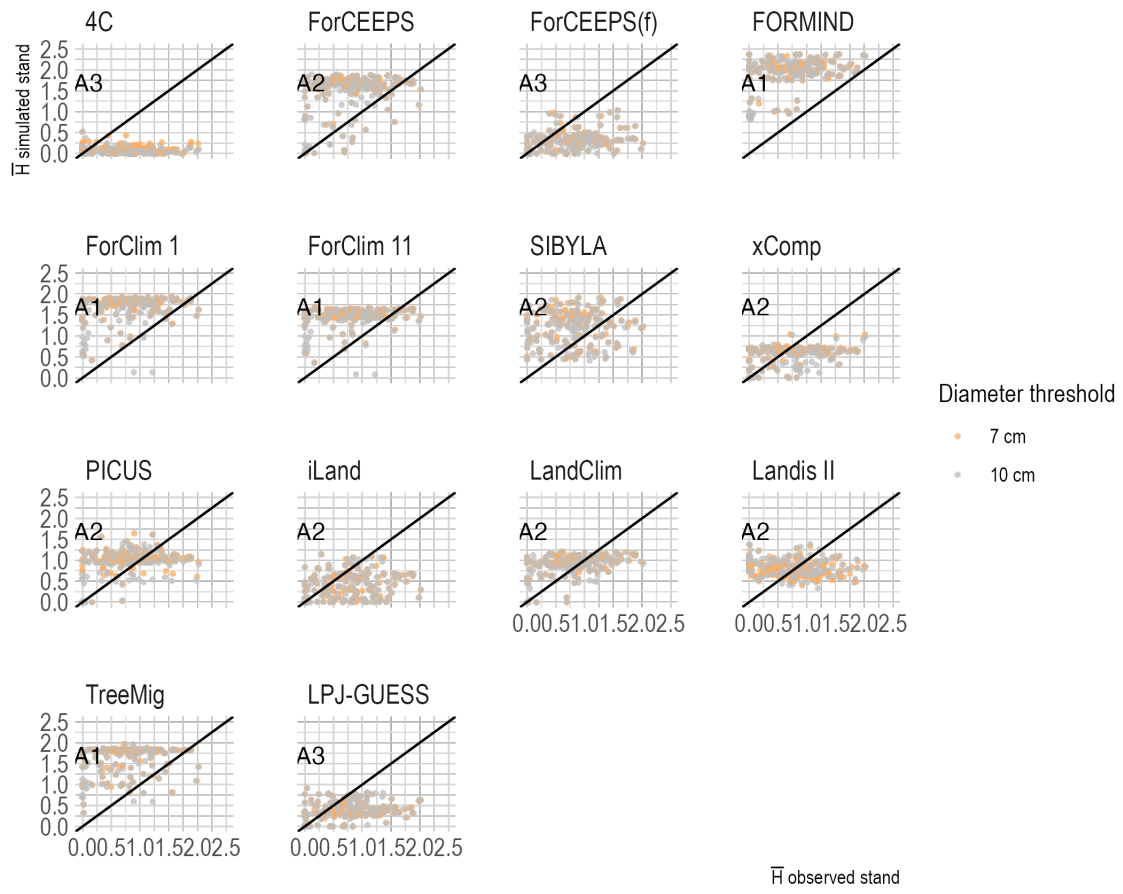


Figure S3: Mean species richness at the stand level per site in the simulated versus observed species richness. The species richness is estimated using the Shannon index calculated by basal area. A1) groups models where the simulated species composition in adults is higher than the observed, A2) groups models where the simulated species composition in adults is similar to the observed, A3) groups models where the simulated species composition in adults is lower than the observed. NOTE: The recruitment threshold recruitment for threshold 7 cm in the empirical data has several sites with no recruitment or no data and the Shannon index for those sites is NA

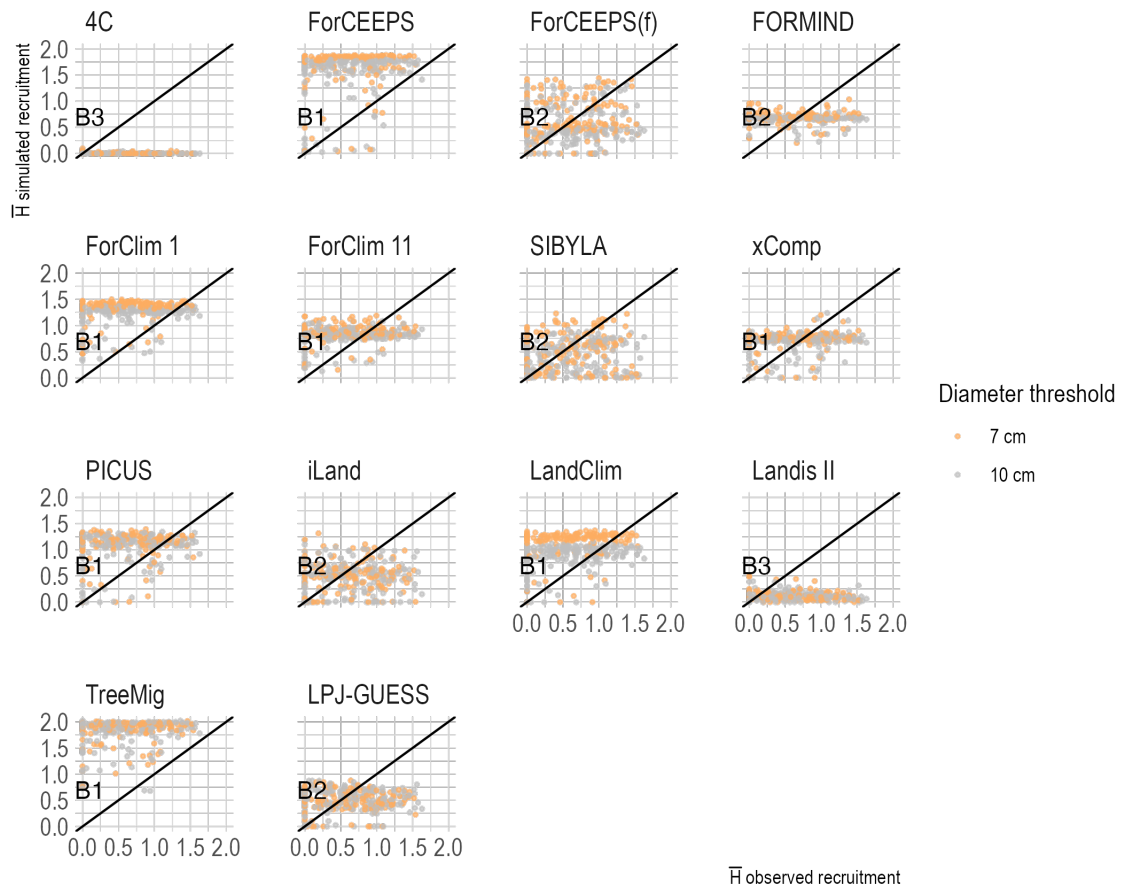


Figure S4: Mean species richness per site in the simulated recruitment versus observed species richness in the recruitment. The species richness is estimated using the Shannon index using the basal area. B1) groups models where the simulated species composition in recruitment is higher than the observed, A2) groups models where the simulated species composition in recruitment is similar to the observed, A3) groups models where the simulated species composition in recruitment is lower than the observed. NOTE: The recruitment threshold recruitment for threshold 7 cm in the empirical data has several sites with no recruitment or no data and the Shannon index for those sites is NA

Table S3: Test of the significance of the differences of rate of recruitment at 7 cm threshold over 10 cm threshold between the observed values and the simulated values per model.

.y.	group1	group2	p	p.adj	p.format	p.signif	method
nn710	Observed	4C	0.0029101	0.02300	0.00291	**	T-test
nn710	Observed	ForCEEPS	0.8983518	1.00000	0.89835	ns	T-test
nn710	Observed	ForCEEPS(f)	0.0253484	0.18000	0.02535	*	T-test
nn710	Observed	FORMIND	0.0599409	0.36000	0.05994	ns	T-test
nn710	Observed	ForClim 1	0.5961405	1.00000	0.59614	ns	T-test
nn710	Observed	ForClim 11	0.2516446	0.75000	0.25164	ns	T-test
nn710	Observed	SIBYLA	0.0001381	0.00150	0.00014	***	T-test
nn710	Observed	xComp	0.0000000	0.00000	1.7e-15	****	T-test
nn710	Observed	PICUS	0.0000000	0.00000	< 2e-16	****	T-test
nn710	Observed	iLand	0.0763056	0.38000	0.07631	ns	T-test
nn710	Observed	LandClim	0.0000770	0.00092	7.7e-05	****	T-test
nn710	Observed	Landis II	0.0002095	0.00210	0.00021	***	T-test
nn710	Observed	TreeMig	0.0000000	0.00000	5.7e-10	****	T-test
nn710	Observed	LPJ-GUESS	0.0013718	0.01200	0.00137	**	T-test
nn710	Observed	aDGVM2	0.1399178	0.56000	0.13992	ns	T-test

Table S4: Models trends in mortality between 7 and 10cm, and the ingrowth at 7cm, based in the mean oer site .

model	Slope	Significance
Observed	0.0037753	0.0279745
4C	0.0054194	0.0144707
ForCEEPS	0.0010021	0.0008576
ForCEEPS(f)	0.0009907	0.0000000
FORMIND	0.0014378	0.4006453
ForClim 1	0.0007425	0.2244471
ForClim 11	-0.0015530	0.0000009
SIBYLA	0.0537439	0.0000001
xComp	0.0034694	0.0000000
PICUS	0.0066061	0.0000000
iLand	0.0026891	0.0000000
LandClim	-0.0028046	0.0000000
Landis II	0.0340037	0.0001270
TreeMig	0.0005776	0.0090166
LPJ-GUESS	0.0021195	0.0017540
aDGVM2	1.6129755	0.3680442

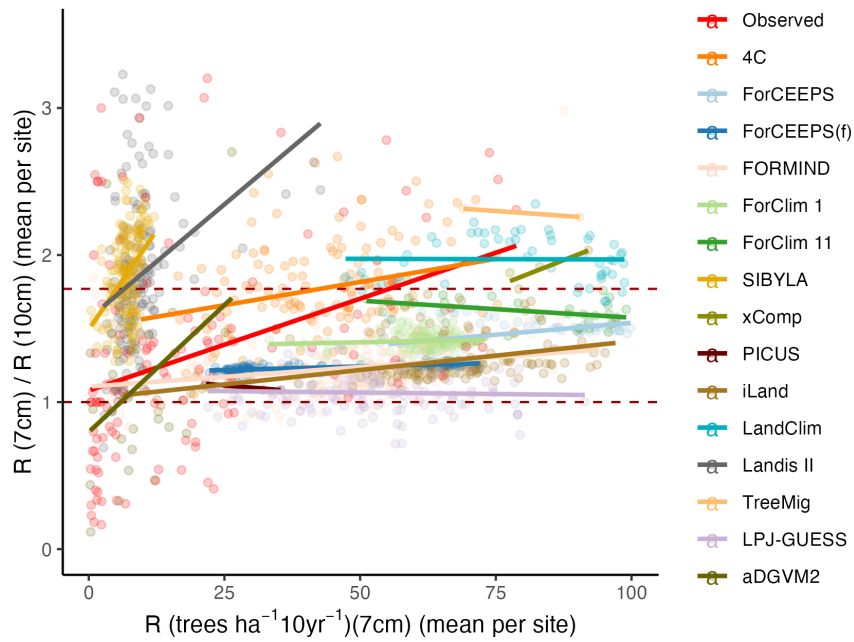


Figure S5: Recruitment ratio between 7 and 10cm and the initial recruitment tree number at 7cm. Dashed red lines mark a ratio equal to 1 indicating no decrease between 7 and 10cm tree recruitment and ratio equal to 1.77 corresponding with the Reineke self-thinning ratio under evenaged conditions

## 1175 2.2 Model traits and model performance

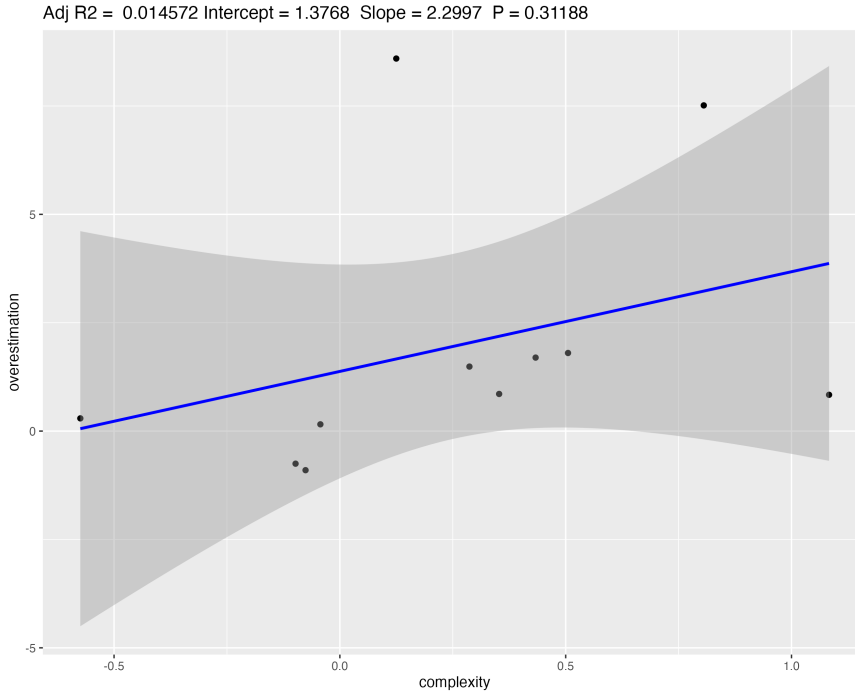


Figure S6: Plot and summary statistics of the linear model between the overestimation proportion in ingrowth levels and the mean complexity value of the establishment modules

Table S5: Test of the significance of the differences of rate of recruitment at 7 cm threshold of the observed values and the simulated values per model.

.y.	group1	group2	p	p.adj	p.format	p.signif	method
r.trees	Observed	4C	0.4154356	4.2e-01	0.42	ns	T-test
r.trees	Observed	ForCEEPS	0.0000000	0.0e+00	< 2e-16	****	T-test
r.trees	Observed	ForCEEPS(f)	0.0000007	2.0e-06	6.8e-07	****	T-test
r.trees	Observed	FORMIND	0.0000021	4.3e-06	2.1e-06	****	T-test
r.trees	Observed	ForClim 1	0.0000000	0.0e+00	< 2e-16	****	T-test
r.trees	Observed	ForClim 11	0.0000000	0.0e+00	< 2e-16	****	T-test
r.trees	Observed	SIBYLA	0.0000000	0.0e+00	< 2e-16	****	T-test
r.trees	Observed	xComp	0.0000000	0.0e+00	< 2e-16	****	T-test
r.trees	Observed	PICUS	0.0000000	0.0e+00	< 2e-16	****	T-test
r.trees	Observed	iLand	0.0000000	0.0e+00	< 2e-16	****	T-test
r.trees	Observed	LandClim	0.0000000	0.0e+00	< 2e-16	****	T-test
r.trees	Observed	Landis II	0.0000000	0.0e+00	< 2e-16	****	T-test
r.trees	Observed	TreeMig	0.0000000	0.0e+00	< 2e-16	****	T-test
r.trees	Observed	LPJ-GUESS	0.0000000	0.0e+00	< 2e-16	****	T-test
r.trees	Observed	aDGVM2	0.0000000	0.0e+00	< 2e-16	****	T-test

Table S6: Test of the significance of the differences of rate of recruitment at 7 cm threshold of the observed values and the simulated values per model.

.y.	group1	group2	p	p.adj	p.format	p.signif	method
ShannonIndexRecruit	Observed	4C	0.0000000	0.0000	< 2e-16	****	T-test
ShannonIndexRecruit	Observed	ForCEEPS	0.0000000	0.0000	< 2e-16	****	T-test
ShannonIndexRecruit	Observed	ForCEEPS(f)	0.1785631	0.1800	0.17856	ns	T-test
ShannonIndexRecruit	Observed	FORMIND	0.0737762	0.1500	0.07378	ns	T-test
ShannonIndexRecruit	Observed	ForClim 1	0.0000000	0.0000	< 2e-16	****	T-test
ShannonIndexRecruit	Observed	ForClim 11	0.0000000	0.0000	4.5e-10	****	T-test
ShannonIndexRecruit	Observed	SIBYLA	0.0161000	0.0640	0.01610	*	T-test
ShannonIndexRecruit	Observed	xComp	0.0270897	0.0810	0.02709	*	T-test
ShannonIndexRecruit	Observed	PICUS	0.0000000	0.0000	< 2e-16	****	T-test
ShannonIndexRecruit	Observed	iLand	0.0046237	0.0230	0.00462	**	T-test
ShannonIndexRecruit	Observed	LandClim	0.0000000	0.0000	< 2e-16	****	T-test
ShannonIndexRecruit	Observed	Landis II	0.0000000	0.0000	< 2e-16	****	T-test
ShannonIndexRecruit	Observed	TreeMig	0.0000000	0.0000	< 2e-16	****	T-test
ShannonIndexRecruit	Observed	LPJ-GUESS	0.0006268	0.0038	0.00063	***	T-test

1176 2.3 Total ingrowth and individual species regeneration niches

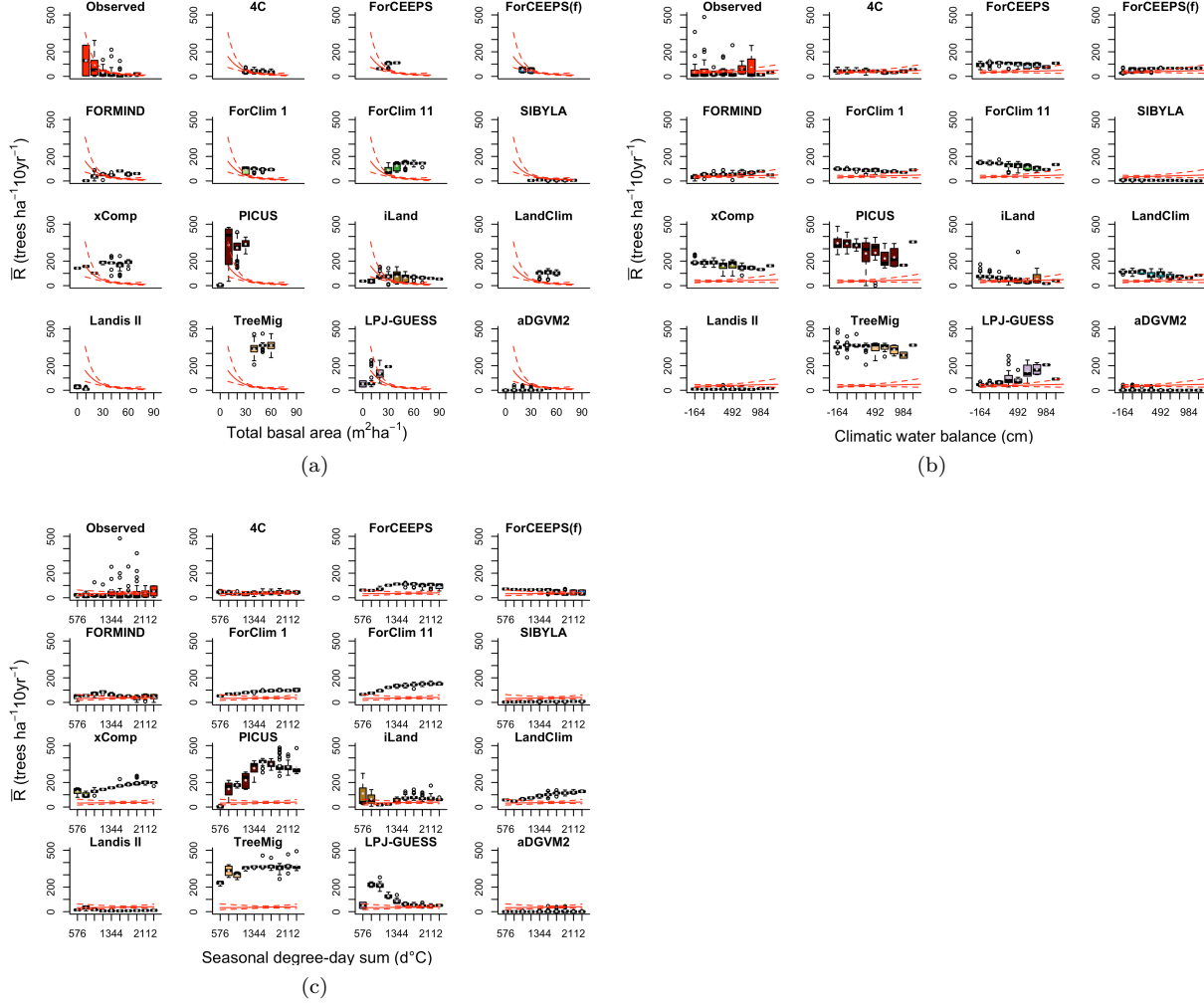


Figure S7: Mean ingrowth values across the 200 samples per site, for the 200 sites against gradients of (a) total basal area; (b) climatic water balance; (c) seasonal degree sum. The values were split into ten bins; the red lines represent a GAM model showing the trend in the observed data.

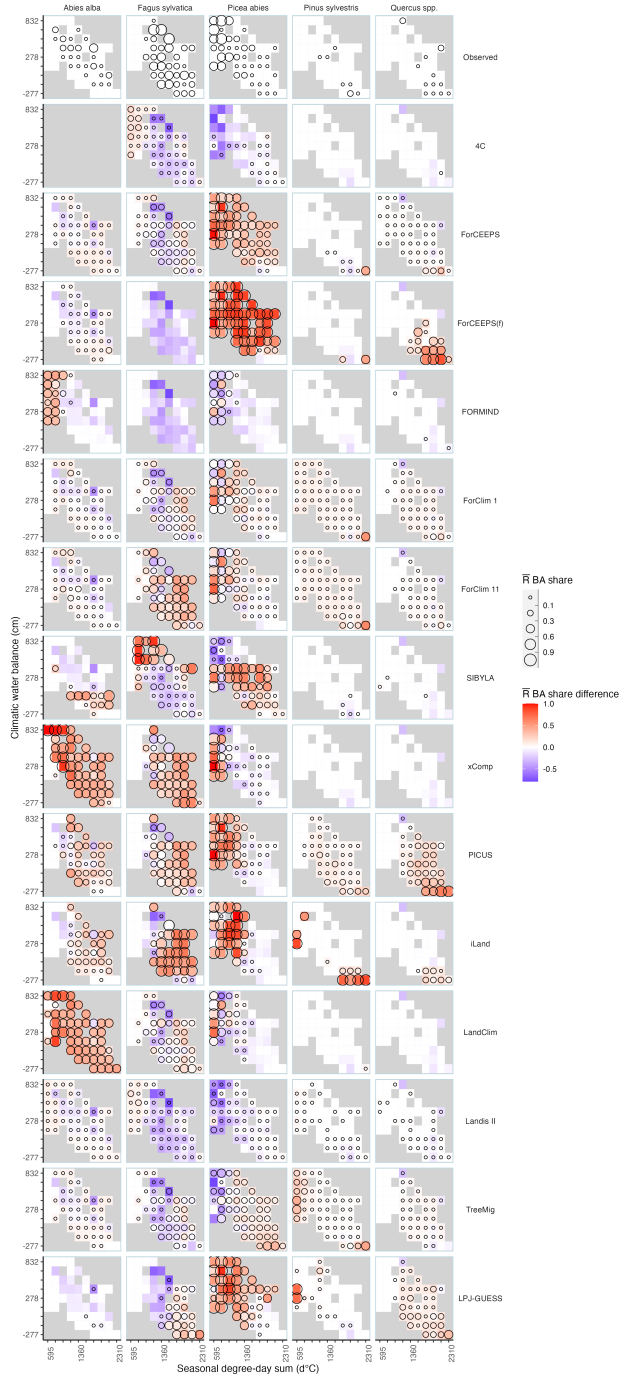


Figure S8: Departure of each model in the representation of the main species recruitment relative abundance from the observations across the environmental gradients for a 10cm treshold. The values shown are the mean of samples per site and across sites in bins, where the range of the climatic water balance (cm) and seasonal degree-day sum ( $d^{\circ}\text{C}$ ) was divided in 10 bins. The point sizes represent ratio between recruited basal area of the species and the total recruited basal area for all the species. The color gradient shows the difference between the simulated and observed ratio between recruited basal area of the species and the total recruited basal area: grey cell represent areas of the environmental gradient in which the model had R BA share and the empirical data did not because both recruitment and stand level recruitments were equal to zero.

<sub>1177</sub> **2.4 References**